
Same places, same stories? Genomics reveals similar structuring and demographic patterns for four *Pocillopora* coral species in the southwestern Indian Ocean

Oury Nicolas ^{1,*}, Mona Stefano ^{2,3}, Magalon H el ene ¹

¹ UMR ENTROPIE (UMR 9220 – Universit e de La R eunion, IRD, IFREMER, Universit e de Nouvelle-Cal edonie, CNRS) Universit e de La R eunion, St Denis La R eunion ,France

² ISYEB – Institut de SYst ematique,  volution, Biodiversit e (UMR 7205 – CNRS, MNHN, Sorbonne Universit e, EPHE, Universit e des Antilles),  cole Pratique des Hautes  tudes Paris ,France

³ EPHE, PSL Research University Paris,France

* Corresponding author : Nicolas Oury, email address : nicolasoury@hotmail.fr

Abstract :

Aim

Efficiently protecting species requires knowing their ecological, life-history and reproductive traits. This is particularly decisive for scleractinian corals, key components of coral reefs, which are experiencing critical declines. Yet their connectivity remains insufficiently documented. Here, we focused on four distinct species of the coral genus *Pocillopora* found in diverse habitats of the southwestern Indian Ocean and presenting various reproductive strategies. We aimed to understand whether these traits affect species connectivity.

Location

Archipelagos and islands of the southwestern Indian Ocean.

Taxon

Pocillopora spp.

Methods

We used target capture to collect single-nucleotide polymorphisms (SNPs) from over a thousand colonies sampled across nine localities. From the ca. 1400 SNPs retained per species, Bayesian clustering methods, networks and demographic inferences were applied to first infer the population genetic structure and connectivity of each species, then the demographic history of each population.

Results

All four *Pocillopora* species exhibited almost the same genetic structuring pattern, reflecting the sampled ecoregions (Madagascar and surrounding islands vs. Mascarene Islands). However, the genetic differentiation was stronger (F_{ST} about 10 times higher) for *P. acuta*, the species inhabiting more enclosed habitats, such as lagoons and shallow waters, and reproducing mainly asexually. Similarly, all populations, except those from *P. acuta*, showed a signature of population expansion ca. 100,000 years ago, following the penultimate glacial period.

Main Conclusions

These results indicate reduced gene flow between Madagascar and the Mascarene Islands, probably linked to currents, suggesting distinct connectivity networks that should be considered independently when setting up conservation plans. In addition, shared demographic histories reflect that populations from these species have probably met the same environmental constraints and reacted similarly, something that should be considered in light of the ongoing rapid climate change.

Keywords : Bayesian assignment, demographic inference, genetic connectivity, Indian Ocean, scleractinian, single-nucleotide polymorphism, target capture, ultraconserved element

67 **SIGNIFICANCE STATEMENT**

68 *Pocillopora* corals are widely distributed through the Indo-Pacific and play crucial roles in reef
69 ecosystems' functioning. Yet, some species remain understudied both in terms of genetic connectivity
70 and evolution, mainly due to species delimitation issues within the genus. Here, based on a panel of
71 genome-wide SNPs, we assessed the population connectivity of four species abundantly found in the
72 southwestern Indian Ocean and inferred their demographic histories. We revealed similar genetic
73 structuring patterns and demographic histories among species, reflecting weak connectivity between
74 Madagascar and the Mascarene Islands, partly due to currents.

75 **INTRODUCTION**

76 Efficiently protecting species requires knowing their ecological, life history and reproductive traits
77 (Clark, 1993). When organisms are difficult to access or when some key processes (e.g., mating, gene
78 flow) are cryptic, such as for marine benthic species, population genetics appears useful to infer
79 population structure and connectivity, but also evolutionary histories (e.g., Maggioni et al., 2020;
80 Padovan et al., 2020). Gathering such data appears crucial to assess evolutionary potential and long-
81 term conservation of species under ongoing changing environments (Gray, 1997).

82 Scleractinian corals, the cornerstone of coral reefs, have experienced critical declines since the
83 1980s (Eddy, Cheung, & Bruno, 2018), making them one of the top science and conservation
84 priorities globally. Yet, the connectivity among their populations, and even more so their evolutionary
85 history, remain insufficiently documented.

86 One of the scleractinian genera whose connectivity is relatively well-documented is the genus
87 *Pocillopora* (e.g., De Palmas, Soto, Ho, Denis, & Chen, 2021; Gélín, Fauvelot, et al., 2017; Gélín,
88 Pirog, Fauvelot, & Magalon, 2018; Magalon, Adjeroud, & Veuille, 2005; Oury, Gélín, & Magalon,
89 2020, 2021; Ridgway, Riginos, Davis, & Hoegh-Guldberg, 2008; Robitzch, Banguera-Hinestroza,
90 Sawall, Al-Sofyani, & Voolstra, 2015; Souter, Henriksson, Olsson, & Grahn, 2009; Torres, Forsman,
91 & Ravago-Gotanco, 2020). Its colonies, abundantly distributed throughout the Indo-Pacific and the
92 Red Sea, are the main bioconstructors in some reefs (e.g., Benzoni, Bianchi, & Morri, 2003). Previous
93 literature assumed that several species (e.g., *P. damicornis*, *P. meandrina*, *P. verrucosa*) were widely
94 distributed throughout the range of the genus (Veron, 2000). However, recent investigations
95 suggested a deep lack of connectivity between both sides of the Indo-Pacific (Gélín, Fauvelot, Bigot,
96 Baly, & Magalon, 2018; Gélín, Pirog, et al., 2018; Oury et al., 2021), to the point that different species
97 could be considered (Gélín, Postaire, Fauvelot, & Magalon, 2017; Oury, Noël, Mona, Aurelle, &
98 Magalon, 2023). The last decades were characterised by a growing number of studies multiplying the
99 methods and lines of evidence to explore species limits within the genus *Pocillopora* (e.g., Gélín,
100 Postaire, et al., 2017; Johnston et al., 2017; Oury et al., 2023; Pinzón et al., 2013; Schmidt-Roach,
101 Miller, Lundgren, & Andreakis, 2014), and move towards an integrative taxonomic revision.

102 Using species delimitation methods based on sequence data from colonies sampled in three
103 marine provinces (western Indian Ocean, tropical southwestern Pacific and south-east Polynesia),
104 Gélín, Postaire, et al. (2017) defined 16 primary species hypotheses (PSHs *sensu* Pante et al., 2015)
105 within the genus *Pocillopora*. Species boundaries were then refined using 13 microsatellite markers
106 and genetic assignment tests, leading to the definition of secondary species hypotheses (SSHs *sensu*
107 Pante et al., 2015) and clusters (Gélín, Postaire, et al., 2017; Gélín, Fauvelot, et al., 2017, 2018; Gélín,
108 Pirog, et al., 2018; Oury et al., 2020, 2021; Oury, Gélín, Rajaonarivelo, & Magalon, 2022). Then,
109 from a subset of individuals representative of each PSH, SSH and cluster, 21 genomic species
110 hypotheses (GSHs) were defined based on genome-wide single-nucleotide polymorphisms (SNPs)
111 (Oury et al., 2023). These GSHs were compared to other lines of evidence in an integrative approach,
112 leading to the definition of 13 strongly supported species, three of which potentially represent species
113 complexes. Most of the colonies from the southwestern Indian Ocean (SWIO) studied therein were
114 attributed to GSH05c-1, GSH05c-2 and GSH05d (all three corresponding to *P. acuta* species

115 complex), GSH09a (*Pocillopora* aff. *P. meandrina*, called *P. eydouxi* in the region but
116 morphologically and genetically closer to *P. meandrina*; see Oury et al., 2023), GSH13a (*Pocillopora*
117 aff. *P. verrucosa*) and GSH13b (*P. villosa nomen nudum*). Hereafter, to lighten the writing, these four
118 species will be referred to as *P. acuta*, *P. aff. meandrina*, *P. aff. verrucosa* and *P. villosa*,
119 respectively.

120 Although accurate knowledge of these species ecology is still lacking, they present different
121 reproductive strategies (with or without clonal propagation; Gélin, Fauvelot, et al., 2017; Oury, Gélin,
122 Massé, & Magalon, 2019; Schmidt-Roach, Lundgren, et al., 2012) and colonise different, more or
123 less open, and/or shallow habitats (e.g., lagoons vs. outer reef slopes; Oury et al., 2023; Schmidt-
124 Roach et al., 2014; Veron, 2000). All four species are sexual broadcast spawners (Schmidt-Roach,
125 Miller, Woolsey, Gerlach, & Baird, 2012), with different timings depending on locality (e.g.,
126 Bouwmeester, Coker, Sinclair-Taylor, & Berumen, 2021; Buck-Wiese et al., 2018; Kruger &
127 Schleyer, 1998), but only *P. acuta* has been reported as an asexual brooder with no doubt (Oury et
128 al., 2019). This latter species seems also more proponent of fragmentation due to its finer branches,
129 and is mostly found in shallow (< 5 m depth) and relatively enclosed habitats compared to other
130 species (Veron, 2000).

131 Different patterns of genetic connectivity might thus be expected for these species, since
132 previous studies have shown more restricted connectivity in brooding corals compared to broadcast
133 spawners (e.g., Thomas et al., 2020; van der Ven, Heynderickx, & Kochzius, 2021), related to,
134 amongst other things, differential planktonic larval durations and behaviours (Coelho & Lasker,
135 2016). As such, genetic connectivity has already been studied among populations of these four species
136 in the SWIO using allozymes (Ridgway, Hoegh-Guldberg, & Ayre, 2001) or microsatellites (Gélin,
137 Fauvelot, et al., 2018, 2017; Gélin, Pirog, et al., 2018; Oury et al., 2021; Ridgway et al., 2008; Souter
138 et al., 2009). Different structuring patterns were found depending on the species and the genetic
139 markers (see Appendix S1, Table S1.1 in Supporting Information for a summary and the
140 correspondences with previous studies): while a general high connectivity was reported for
141 *P. aff. verrucosa* and *P. villosa* using 13 microsatellites (Oury et al., 2021), a strong genetic
142 differentiation was found within *P. acuta* with the same 13 microsatellites, which may be related to
143 its different reproductive strategy (Gélin, Pirog, et al., 2018). However, for *P. aff. meandrina*, the
144 same 13 microsatellites highlighted the presence of three sympatric clusters found in relatively similar
145 proportions in all sampled sites, and the connectivity was high within each cluster (Gélin, Fauvelot,
146 et al., 2018; Oury et al., 2021). This diversity of patterns found within the same region and within
147 congeneric species, some of which adopt the same reproductive strategy, seems surprising and
148 questions the origin of such differences.

149 Here, to confirm or refute previous genetic structuring patterns found in these four *Pocillopora*
150 species from the SWIO, we used target-capture of ultraconserved elements (UCEs) and exon loci,
151 from over a thousand colonies, to collect a panel of genome-wide SNPs. Bayesian clustering methods,
152 networks and demographic inferences were applied to infer the population genetic structure and
153 connectivity of each species, but also the demographic history of each population. Through a multi-
154 species approach, these results provide insights for a better understanding of the evolutionary history

155 of these species, as well as the connectivity pattern in the SWIO. Ultimately, this will allow the
 156 implementation of effective conservation measures in a context of coral decline.

157

158 MATERIALS AND METHODS

159

160 Sampling

161 The sampling was the same as in our previous studies (e.g., Oury et al., 2022), but focusing only on
 162 colonies from the southwestern Indian Ocean (SWIO). It represents ca. 5,000 *Pocillopora* colonies
 163 sampled within more than 40 sites from 11 localities. All colonies were previously genotyped with
 164 13 microsatellites and a subset (ca. 10%) was also amplified for the mitochondrial open reading frame
 165 marker (mtORF). Based on these genetic data, each colony was assigned beforehand to a primary and
 166 a secondary species hypothesis (PSH and SSH, respectively; *sensu* Gélín, Postaire, et al., 2017), and
 167 a cluster when appropriate. Here, to further study the genetic structure of the four targeted species
 168 (i.e., *P. acuta*, *P. aff. meandrina*, *P. aff. verrucosa* and *P. villosa*), we sequenced, when possible, a
 169 subset of at least 20 colonies per locality and per genetic cluster. Accordingly, 1,023 *Pocillopora*
 170 colonies from 35 sites and nine localities were considered (Table 1; Fig. 1; see Appendix S2,
 171 Table S2.2).

172

173 **Table 1** Sampling localities of *Pocillopora* colonies (see Appendix S2, Table S2.2 in Supporting Information
 174 for details per site). N_{sites} : number of sites sampled; N , N_L , N_{acuta} , N_{meand} , N_{verru} and N_{villo} : total numbers of
 175 sampled colonies, of clonal lineages and of colonies assigned to *P. acuta*, *Pocillopora* aff. *P. meandrina*,
 176 *Pocillopora* aff. *P. verrucosa* and *P. villosa nomen nudum*, respectively; R : clonal richness (Dorken & Eckert,
 177 2001). Two *P. acuta* colonies from northwestern Madagascar (MADnw) were removed due to missing data
 178 and are not counted here.

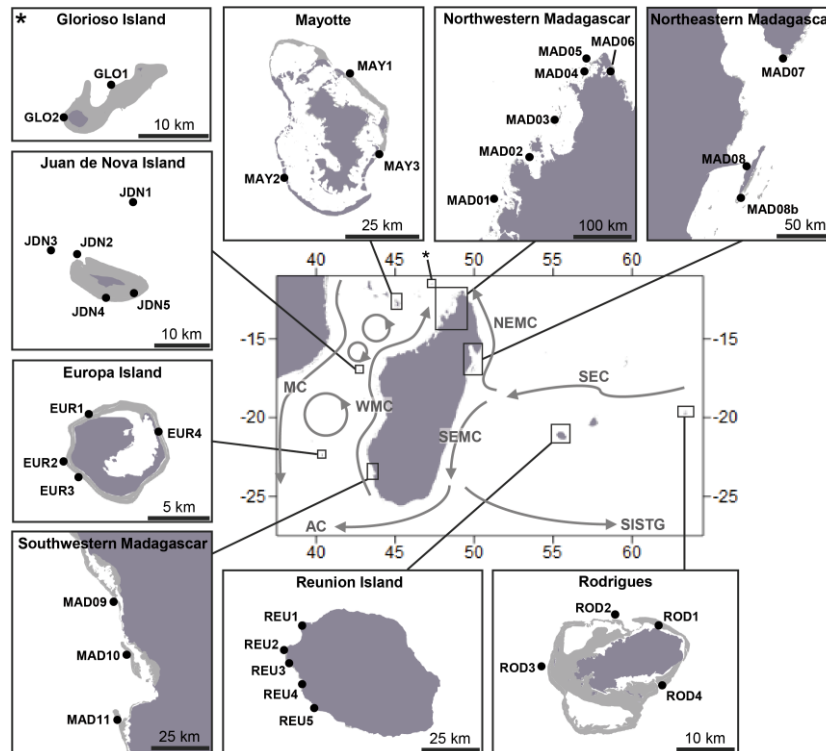
Ecoregion	Island/Region	Code	Latitude	Longitude	N_{sites}	N	N_{acuta}	N_{meand}	N_{verru}	N_{villo}	
	Mayotte	MAY	-12.83131	45.16044	3	153	30	85	20	18	
	Glorioso Island	GLO	-11.56377	47.29394	2	10	0	6	2	2	
Western and Northern Madagascar	Juan de Nova Island	JDN	-17.04855	42.72176	5	148	48	77	21	2	
	Europa	EUR	-22.36783	40.37185	4	81	0	46	20	15	
	Northwestern Madagascar	MADnw	-16.18321	49.94950	6	118	43	48	23	4	
	Northeastern Madagascar	MADne	-13.46366	48.25272	3	60	4	6	35	15	
	Southwestern Madagascar	MADse	-23.47539	43.66148	3	141	24	76	21	20	
Mascarene Islands	Reunion Island	REU	-21.16115	55.57841	5	176	65	72	20	19	
	Rodrigues	ROD	-19.69775	63.44172	4	134	27	80	20	7	
					N	35	1021	241	496	182	102
					N_L	-	850	95	490	179	86
					R	-	0.83	0.39	0.99	0.98	0.84

179

180 Laboratory and preliminary bioinformatics steps

181 Total genomic DNA was extracted using the DNeasy® Blood & Tissue kit (QIAGEN GmbH, Hilden,
 182 Germany), according to manufacturer protocol. Samples were then PE150 sequenced with an
 183 Illumina NovaSeq 6000 (Illumina, San Diego, CA) at the platform iGenSeq (ICM, Paris, France),
 184 following a capture protocol targeting 1,248 ultraconserved elements (UCEs) and 1,385 exon loci
 185 (Cowman et al., 2020), as in Oury et al. (2023). Seven haphazardly chosen samples were
 186 independently prepared and sequenced twice (sequencing replicates) to estimate the sequencing error
 187 rate, and the variant calling and filtering accuracy. After sequencing, reads were processed as in Oury

188 et al. (2023) and mapped to the 2,068 reference sequences constructed *de novo* therein (available at
 189 <https://doi.org/10.5281/zenodo.7885458>).
 190



191 [2/3rd column] **Figure 1** Sampling localities of *Pocillopora* colonies (dark and light greys indicate lands and
 192 coral reefs, respectively). Sites are numerically identified from the island code: GLO: Glorioso Islands, MAY:
 193 Mayotte, MAD: Madagascar, JDN: Juan de Nova Island, EUR: Europa Island, REU: Reunion Island and ROD:
 194 Rodrigues. Major oceanic currents are indicated schematically: MC: Mozambique current, WMC: west
 195 Madagascar current, AC: Agulhas current, NEMC: north-east Madagascar current, SEMC: south-east
 196 Madagascar current, SEC: south equatorial current and SISTG: south Indian subtropical gyre (Hancke,
 197 Roberts, & Ternon, 2014; Lutjeharms & Bornman, 2010; Schott & McCreary Jr, 2001).
 198

199 **Species identification of the colonies**

200 To verify the identification of the colonies in the light of recent genomic investigations (Oury et al.,
 201 2023), a first dataset was constructed by calling the genotypes of each sample for the 1,559 SNPs that
 202 were used for species delimitation in Oury et al. (2023; see Appendix S3 for more details). A single
 203 representative of each sequencing replicate (the one with the least missing data) was kept.

204 Assignment tests were then performed with sNMF (Frichot, Mathieu, Trouillon, Bouchard, &
 205 François, 2014), implemented in the R v4.0.4 (R Core Team, 2021) library ‘LEA’ (Frichot & François,
 206 2015). Besides, 167 of the 1,023 colonies considered in this study (16%) were previously used in the
 207 genomic species delimitation analyses from Oury et al. (2023), and their corresponding genomic
 208 species hypotheses (GSHs) are thus known. sNMF was first run with these 167 colonies only, to
 209 retrieve the GSHs, then including all 1,023 colonies. Five repetitions per *K* were run, with *K* varying
 210 from 2 to 10. Results were visualised with CLUMPAK (Kopelman, Mayzel, Jakobsson, Rosenberg, &
 211 Mayrose, 2015), and used to identify colonies to the species level (see Results). A principal
 212 component analysis (PCA) including all 1,023 colonies was also performed with the R library
 213 ‘adeigenet’ (Jombart, 2008).
 214

215 **Population structure and connectivity**

216 *Datasets construction*

217 Once species were identified, four separate datasets (one for each species) were distinguished,
218 from which SNPs were recalled from the individual bam files to get a more accurate genotyping (see
219 Appendix S3 for more details). Tri- and tetra-allelic sites, as well as sites presenting more than 20%
220 of missing data and sites with a minor allele frequency (MAF) inferior to 0.05 were discarded. Two
221 *P. acuta* individuals presenting high proportions of missing data (> 75%) were removed. Then, one
222 SNP was randomly chosen per locus to reduce the effect of linkage disequilibrium, resulting in the
223 four datasets that were used for subsequent analyses.

225 *Clonal lineages identification*

226 Clonal lineages (i.e., groups of genetically related individuals resulting from asexual reproduction)
227 were identified by computing the genetic distance [number of different alleles estimated with the
228 *diss.dist* function from the R library ‘*poppr*’ (Kamvar, Tabima, & Grünwald, 2013) over number of
229 sites genotyped for both individuals] between all pairs of individuals within each dataset. The
230 distribution of these genetic distances among individuals was then plotted and the first antimode was
231 defined as the threshold separating individuals belonging to the same clonal lineage (smaller distances
232 between individuals) from those belonging to different clonal lineages (larger distances between
233 individuals). Sequencing replicates were used to help position the threshold. Clonal lineages were
234 then visualised in R with a hierarchical clustering of the individuals based on genetic distances. The
235 clonal richness (R ; Dorken & Eckert, 2001) of each dataset was then calculated as $\frac{N_L-1}{N-1}$, with N and
236 N_L , the total numbers of colonies and clonal lineages in the dataset, respectively.

238 *Structure analyses*

239 All further analyses were performed keeping one representative of each clonal lineage per population,
240 as closely related individuals can bias estimators which are not designed for clonal populations.
241 However, for *P. acuta*, as a significant number of colonies was removed (61%; see Results), and since
242 all colonies theoretically participate equally in sexual reproduction and gene flow, analyses were
243 performed on both a truncated (i.e., keeping one representative of each clonal lineage per population)
244 and an entire (i.e., keeping all individuals) datasets.

245 First, assignment tests were performed with sNMF (Frichot et al., 2014), STRUCTURE v2.3.4
246 (Pritchard, Stephens, & Donnelly, 2000) and discriminant analyses of principal components (DAPC;
247 Jombart, Devillard, & Balloux, 2010). STRUCTURE was run with the admixture model, assuming
248 correlated allele frequencies. Three iterations of 5×10^5 MCMC generations after an initial burn-in
249 of 5×10^4 generations were run for each K , varying from $K = 2$ to $K = 10$. sNMF and DAPC were
250 performed with the R libraries ‘*LEA*’ (Frichot & François, 2015) and ‘*adegenet*’ (Jombart, 2008),
251 respectively. Five repetitions per K , with K varying from 2 to 10, were run for sNMF, with a maximum
252 of 500 iterations before reaching stationarity. Results were STRUCTURE-like plotted for all three
253 assignment methods (i.e., STRUCTURE, sNMF and DAPC) with CLUMPAK (Kopelman et al., 2015), to
254 allow their comparison. Additionally, a principal component analysis (PCA) was performed with the

255 R library ‘*adegenet*’ (Jombart, 2008). Nei (1972) individual genetic distances were estimated with
256 the R library ‘*StAMPP*’ (Pembleton, Cogan, & Forster, 2013), and were used to build a minimum
257 spanning tree (MST) and an unrooted equal-angle split network, with EDENETWORKS v2.18 (Kivelä,
258 Arnaud-Haond, & Saramäki, 2015) and SplitsTree v4.15.1 (Huson & Bryant, 2006), respectively.

259 Finally, once the number of clusters defined for each species, a population was considered as
260 all colonies sampled in the same site and assigned to the same cluster according to the three
261 assignment methods (i.e., sNMF, STRUCTURE and DAPC). Populations with less than 10 individuals
262 were not retained for further analyses, but some sites were pooled together as a single population to
263 achieve larger population sizes (Fig. 2; see Appendix S2, Table S2.2). Since this pooling of
264 populations may affect the results of some analyses, the distance between pooled sites was limited to
265 a few tens of kilometres and results were interpreted carefully. F_{ST} (Weir & Cockerham, 1984) were
266 computed with the R library ‘*StAMPP*’ (Pembleton et al., 2013) for each pair of conspecific
267 populations.

268

269 *Direction and barrier to gene flow*

270 Directional gene flow among populations was assessed by constructing a relative migration network
271 with *divMigrate* (Sundqvist, Keenan, Zackrisson, Prodöhl, & Kleinhans, 2016), implemented in the
272 R library ‘*diveRsity*’ (Keenan, McGinnity, Cross, Crozier, & Prodöhl, 2013). Analyses were run for
273 all populations within each species using the G_{ST} (Nei, 1973) and 1,000 bootstraps, and by
274 incrementing the filter threshold (t) by 0.05 until the network becomes fragmented.

275 Then, geographic areas with pronounced genetic discontinuity between populations were
276 identified with the Barrier v2.2 program (Manni, Guérard, & Heyer, 2004). The geographical
277 coordinates and genetic distances (Nei, 1972) were thus connected by Delauney triangulation such
278 that each connection had an associated distance, and barriers were identified using a Monmonier
279 (1973) maximum distance algorithm. Barrier support was assessed through 1,000 distance matrices
280 bootstrapped over loci.

281

282 *Isolation by distance × environment*

283 To explore the effect of distance and environment on the population structure among all four species,
284 a factorial analysis of mixed data (FAMD) was performed using the R library ‘*FactoMineR*’ (Lê,
285 Josse, & Husson, 2008). Within-species pairwise population F_{ST} and shortest distances at sea
286 (computed with QGIS v2.18.28; <http://www.qgis.org>) were used as measures of population structure
287 and geographic distance, respectively. Environmental layers (present mean surface temperature,
288 salinity, current velocity and chlorophyll concentration) were downloaded from Bio-ORACLE v2.2
289 (Assis et al., 2018) and queried with the population site coordinates using the R libraries
290 ‘*sdmpredictors*’ (Bosch & Fernandez, 2023) and ‘*raster*’ (Hijmans, 2023). From the data extracted
291 for each environmental layer, two statistics were then calculated per population pair: the mean and
292 the difference, resulting in eight environmental variables. Finally, to account for species intrinsic
293 differences (e.g., reproduction strategy), a qualitative variable “species” was included in the analysis.

294 Mantel (1967) tests were also performed in R to evaluate the correlation between F_{ST} and shortest
295 distances at sea among populations for each species and each cluster separately.

296

297 **Past effective population sizes**

298 For each population, to infer population demographic histories, site allele frequency likelihoods were
299 generated with ANGSD v0.935 (Korneliussen, Albrechtsen, & Nielsen, 2014), directly from the
300 individual bam files. Genotype likelihoods were computed using the samtools method (-GL 1; Li et
301 al., 2009), requiring a mapping quality (minMapQ) and a base quality (minQ) of at least 30 and 20,
302 respectively, and considering only sites with no missing data (see Appendix S3, Table S3.3). From
303 that, the folded site frequency spectrum (SFS) was estimated using REALSFS (Nielsen, Korneliussen,
304 Albrechtsen, Li, & Wang, 2012). Past variations in effective population sizes (N_e) were reconstructed
305 using Stairway Plot v2.1 (Liu & Fu, 2020) from the folded SFS, both keeping or discarding
306 singletons. Generation time was assumed to be five years for each species, as in *Acropora* (Mao,
307 Economo, & Satoh, 2018; Matz, Treml, Aglyamova, & Bay, 2018), regarding their relatively similar
308 life history traits (e.g., fast growth and maturity). Likewise, the mutation rate per site and per
309 generation was set to 3×10^{-8} (Mao et al., 2018).

310

311 **RESULTS**

312 A total of 1,023 *Pocillopora* colonies were sequenced (plus seven sequencing replicates), leading to
313 4.0×10^9 reads (6.1×10^{11} bp), with between 1.7×10^6 and 6.8×10^6 reads per individual
314 [mean \pm s.e. = $(3.9 \pm 0.0) \times 10^6$ reads]. Quality controls and adapter trims then led to the removal of
315 2.6% of the bases. Between 12.1% and 85.4% trimmed reads per individual were successfully mapped
316 on the reference sequences (mean \pm s.e. = $76.8 \pm 0.2\%$; only two individuals had less than 50% of
317 their reads mapped and were removed *a posteriori*), with a mean coverage depth (\pm s.e.) of $48.6 \times$
318 (± 0.1).

319

320 **Species identification**

321 Genotype calling for the 1,559 SNPs used in the species delimitation analyses in Oury et al. (2023)
322 led to a dataset of 1,023 individuals \times 1,559 SNPs, with 4.5% missing data (see Appendix S3,
323 Table S3.4) and a mean SNP coverage depth (\pm s.e.) of $72.4 \times (\pm 1.5)$. Individual proportions of
324 missing data ranged from 0.3% to 35.5%, except for two individuals ($> 75\%$; removed *a posteriori*).

325 sNMF assignments at $K = 4$ grouped all 167 colonies already identified in Oury et al. (2023) to
326 a cluster corresponding to their respective species (i.e., *P. acuta*, *P. aff. meandrina*, *P. aff. verrucosa*
327 or *P. villosa*), with few admixture [mean (\pm s.e.) colonies assignment probability to the cluster
328 corresponding to the species = 0.96 ± 0.00], while at $K = 6$, clusters corresponded to the genomic
329 species hypotheses (GSHs), but admixture blurred some clusters boundaries [mean (\pm s.e.) colonies
330 assignment probability to the cluster corresponding to the GSH = 0.89 ± 0.01 ; see Appendix S4,
331 Fig. S4.1]. Accordingly, the PCA with all 1,023 colonies distinguished four groups corresponding to
332 the four species (see Appendix S4, Fig. S4.2). Thus, the remaining colonies were identified to the
333 species level and were considered to belong to a species when they were assigned to the corresponding

334 specific cluster with a probability ≥ 0.9 at $K = 4$. Accordingly, all colonies were identified, with 243
335 colonies assigned to *P. acuta*, 496 to *P. aff. meandrina*, 182 to *P. aff. verrucosa* and 102 to *P. villosa*
336 (Table 1; see Appendix S2, Table S2.2).

337

338 **Population structure and connectivity**

339 SNP calling and filtering for each species separately led to four distinct datasets: *P. acuta*
340 [244 individuals (including three replicates) \times 1,493 SNPs; %NA = 3.9%], *P. aff. meandrina*
341 [497 individuals (including one replicate) \times 1,412 SNPs; %NA = 4.2%], *P. aff. verrucosa*
342 [185 individuals (including three replicates) \times 1,446 SNPs; %NA = 4.1%] and *P. villosa*
343 [102 individuals (no replicate) \times 1,351 SNPs; %NA = 4.6%] (see Appendix S3, Table S3.4).

344

345 *Clonal lineages identification*

346 Over all datasets, sequencing replicates differed by less than 0.5% (see Appendix S5, Fig. S5.3). The
347 histograms of the pairwise distances showed a clear antimode for three species: *P. aff. meandrina*,
348 *P. aff. verrucosa* and *P. villosa*, with no comparison falling between 0.5% and 18-20%. Thus, for
349 these three species, colonies were considered to belong to the same clonal lineage when they differed
350 from less than 1%. Accordingly, one lineage was represented by 11 sympatric colonies in *P. villosa*,
351 and 12 others were represented by two or three sympatric colonies (six in *P. aff. meandrina*, two in
352 *P. aff. verrucosa* and four in *P. villosa*), resulting in clonal richnesses (R) of 0.99, 0.98 and 0.84 for
353 *P. aff. meandrina*, *P. aff. verrucosa* and *P. villosa*, respectively (Table 1; see Appendix S2,
354 Table S2.2). For *P. acuta*, only one comparison fell between 1.3% and 4.9% (see Appendix S5,
355 Fig. S5.3). The threshold was thus defined at 3% so that the colonies diverging from 2.4% belong to
356 the same clonal lineage. Accordingly, a total of 95 different *P. acuta* clonal lineages were detected
357 among the 241 colonies ($R = 0.39$; Table 1; see Appendix S2, Table S2.2), with 51 lineages
358 represented by two to 18 colonies. Five lineages were found at different sampling sites: one in
359 MAD05/MAD06 (distant from 38 km), three in REU3/REU5 (22 km) and one in REU4/REU5
360 (11 km).

361

362 *Structure analyses*

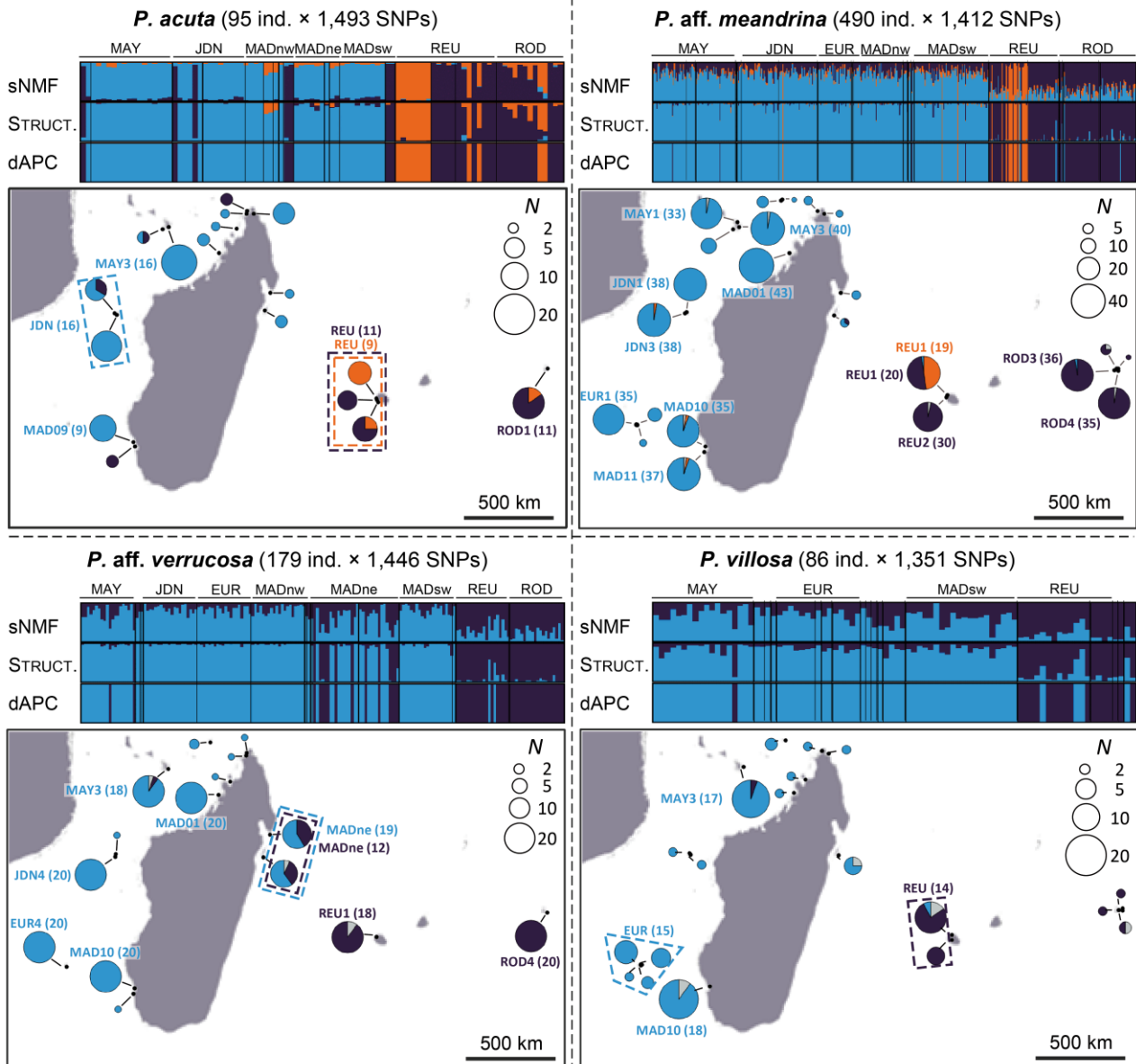
363 Results from the three assignment methods (i.e., sNMF, STRUCTURE and DAPC) were very consistent
364 across each of the four species, at least for the first K values (Fig. 2; see Appendix S6). However,
365 their respective decision criteria [i.e., the cross-entropy for sNMF, the estimated posterior probability
366 LnP(D) for STRUCTURE and the Bayesian information criteria (BIC) for DAPC] supported different
367 most likely K values. Representing mathematical estimates and not always the biological truth, we
368 retained for each species the maximum K for which all methods were congruent, rather than the value
369 suggested by the criteria (which was not always the same).

370 For *P. acuta*, both for the entire and the truncated datasets (see Appendix S6, Fig. S6.4 and
371 S6.5), the three assignment methods were congruent at $K = 2$ and $K = 3$ and retrieved the three GSHs
372 from Oury et al. (2023; i.e., GSH05c-1, GSH05c-2 and GSH05d, corresponding to the orange, purple
373 and blue clusters herein, respectively). From $K = 4$, assignments became incongruent between

374 datasets, but also between methods for the entire dataset, suggesting three clusters for *P. acuta*. The
375 PCA, the MST and the network also retrieved these three clusters (see Appendix S6, Fig. S6.4 and
376 S6.4). All colonies were assigned to one of the three clusters [$N_{blue} = 141$ (55 clonal lineages;
377 $R_{blue} = 0.39$); $N_{purple} = 45$ (29 clonal lineages; $R_{purple} = 0.64$); $N_{orange} = 55$ (11 clonal lineages;
378 $R_{orange} = 0.19$); see Appendix S2, Table S2.2], with a clear ecoregion pattern [95% of the colonies
379 sampled in Madagascar and surrounding islands belong to the blue cluster, while 100% of the colonies
380 sampled in the Mascarene Islands (Reunion and Rodrigues) belong to the purple and orange clusters;
381 Fig. 2; see Appendix S6, Fig. S6.6]. However, this partitioning induced small population sizes,
382 especially for the truncated dataset. F_{ST} between populations were all significantly high ($P < 0.001$),
383 ranging from 0.032*** to 0.332*** for the entire dataset, and from 0.045*** to 0.273*** for the
384 truncated one, but intra-cluster F_{ST} (mean \pm s.e. = 0.129 ± 0.013 and 0.059 ± 0.010 for the entire and
385 truncated datasets, respectively) were generally smaller than inter-cluster ones (0.261 ± 0.007 and
386 0.212 ± 0.009 , respectively; see Appendix S6, Table S6.5a-b and Fig. S6.7). In particular, the highest
387 F_{ST} were found for inter-cluster population pairs involving a population belonging to the purple
388 cluster.

389 For *P. aff. meandrina* (see Appendix S6, Fig. S6.8), three clusters were found by the three
390 assignment methods and the PCA, but the MST and the network only distinguished the orange cluster
391 (Fig. 2; see Appendix S6, Fig. S6.8). All but seven colonies (1%) were assigned to one of the three
392 clusters ($N_{blue} = 335$, $N_{purple} = 126$, $N_{orange} = 22$; see Appendix S2, Table S2.2), with the same
393 geographic pattern as identified for *P. acuta* (99% to the blue cluster in Madagascar vs. 99% to the
394 purple and orange clusters in the Mascarenes; Fig. 2). Thirteen populations were retained for
395 subsequent analyses (Fig. 2). Considering only the blue and purple clusters, F_{ST} ranged from -0.001^{NS}
396 to 0.010***, with significant and higher F_{ST} for inter-cluster comparisons [mean intra-cluster F_{ST}
397 (\pm s.e.) = 0.000 ± 0.000 ; mean inter-cluster F_{ST} (\pm s.e.) = 0.008 ± 0.000]. However, inter-cluster F_{ST}
398 involving the population from the orange cluster were almost 10 times higher (mean \pm s.e. =
399 0.066 ± 0.001 ; see Appendix S6, Table S6.5c and Fig. S6.7).

400 Finally, for *P. aff. verrucosa* and *P. villosa* (see Appendix S6, Fig. S6.9 and S6.10,
401 respectively), results were very similar and suggested two clusters for each species (Fig. 2). Indeed,
402 all three assignment methods were congruent for $K = 2$, while incongruent for $K \geq 3$. The PCA
403 retrieved each cluster, but the MST and the network did not (see Appendix S6, Fig. S6.9 and S6.10).
404 All colonies, except four (2%) for *P. aff. verrucosa* and six (7%) for *P. villosa*, were assigned to one
405 of the two clusters (*P. aff. verrucosa*: $N_{blue} = 124$, $N_{purple} = 51$; *P. villosa*: $N_{blue} = 62$, $N_{purple} = 18$; see
406 Appendix S2, Table S2.2), again according to their ecoregion (*P. aff. verrucosa*: 91% to the blue
407 cluster in Madagascar vs. 100% to the purple cluster in the Mascarenes; *P. villosa*: 98% to the blue
408 cluster in Madagascar vs. 94% to the purple cluster in the Mascarenes; Fig. 2). Nine and four
409 populations were retained for subsequent analyses, for *P. aff. verrucosa* and *P. villosa*, respectively
410 (Fig. 2). F_{ST} were of the same order of magnitude for both species (*P. aff. verrucosa*: $-0.002^{NS} < F_{ST}$
411 $< 0.014^{***}$; *P. villosa*: $-0.003^{NS} < F_{ST} < 0.016^{***}$) and were significantly positive, with inter-cluster
412 F_{ST} being higher [both species: mean intra-cluster F_{ST} (\pm s.e.) = 0.000 ± 0.000 ; mean inter-cluster F_{ST}
413 (\pm s.e.) = 0.011 ± 0.000 ; see Appendix S6, Table S6.4d-e and Fig. S6.7].



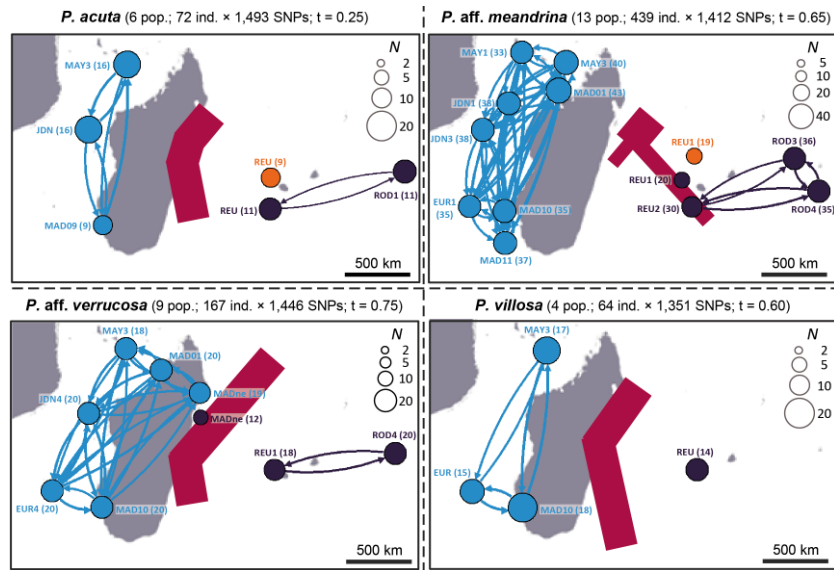
415 [double column] **Figure 2** Population structure of each *Pocillopora* species (i.e., *P. acuta*, *Pocillopora* aff.
 416 *P. meandrina*, *Pocillopora* aff. *P. verrucosa* and *P. villosa nomen nudum*). For each species (numbers of
 417 individuals and SNPs of the corresponding dataset in parentheses), results from the three assignment methods
 418 (sNMF, STRUCTURE and DAPC) at the retained K ($K = 2$ for *P. aff. verrucosa* and *P. villosa*; $K = 3$ for *P. acuta*
 419 and *P. aff. meandrina*) are indicated above, as well as the corresponding cluster repartition below (grey
 420 portions represent individuals not assigned to the same cluster by all methods). Populations retained for further
 421 analyses are labelled (colour refers to the cluster; population size in parentheses). Dashed polygons represent
 422 pooled populations. N : number of colonies; MAY: Mayotte, JDN: Juan de Nova Island, EUR: Europa Island,
 423 MAD: Madagascar (nw: northwestern, ne: northeastern, sw: southwestern), REU: Reunion Island, ROD:
 424 Rodrigues.

425

426 *Direction and barrier to gene flow*

427 The networks of relative migration direction among populations and barrier analyses gave similar
 428 results among species and highlighted reduced gene flow between Madagascar and the Mascarene
 429 Islands, in concordance with the clusters previously delimited. Thus, gene flow among populations
 430 from the same cluster was higher compared to that among populations from different clusters, but
 431 showed no dominant direction (Fig. 3; see Appendix S7, Fig. S7.11). All species but *P. acuta* had a

432 similar filter threshold beyond which the network becomes fragmented ($0.65 \leq t \leq 0.75$ vs. 0.25 for
 433 *P. acuta*; Fig. 3).
 434

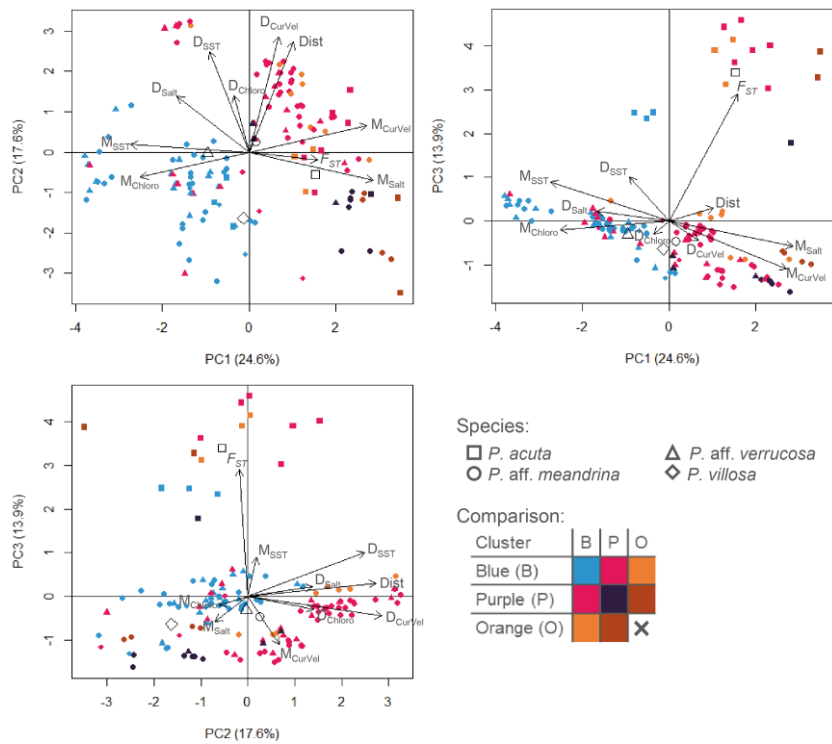


435 [2/3rd column] **Figure 3** Direction and barrier to gene flow for each *Pocillopora* species (i.e., *P. acuta*,
 436 *Pocillopora* aff. *P. meandrina*, *Pocillopora* aff. *P. verrucosa* and *P. villosa nomen nudum*). Populations are
 437 coloured according to clusters. Arrows indicate gene flow above the filter threshold for which the network
 438 becomes fragmented (t ; indicated above, along with the numbers of populations, individuals and SNPs
 439 retained). Note that no arrows do not indicate the absence of gene flow. Red lines symbolise barriers (width
 440 proportional to support over 1,000 bootstrap replicates).
 441

442 *Isolation by distance × environment*

443 The first three principal components (PC1-3) of the FAMD explained 56.1% of the variability
 444 (Fig. 4). PC1 and PC2 separated population pairs of Madagascar (i.e., comparisons within the blue
 445 cluster for each species) from other pairs, in relation with environmental variables, while PC3
 446 separated population pairs based on species (*P. acuta* being more distant), due to F_{ST} . Thus, no
 447 correlation was found between F_{ST} and environmental variables, nor with distances, but rather with
 448 the species variable (accounting for species intrinsic differences; Fig. 4).

449 Mantel tests revealed a significant, but weak, correlation between F_{ST} and shortest distances at
 450 sea for *P. aff. verrucosa* ($N = 36$; $R^2 = 0.291$; $P < 0.001^{***}$) and its blue cluster ($N = 15$; $R^2 = 0.267$;
 451 $P < 0.048^*$). All other correlations were not significant ($P > 0.05^{NS}$; see Appendix S8, Fig. S8.12).
 452



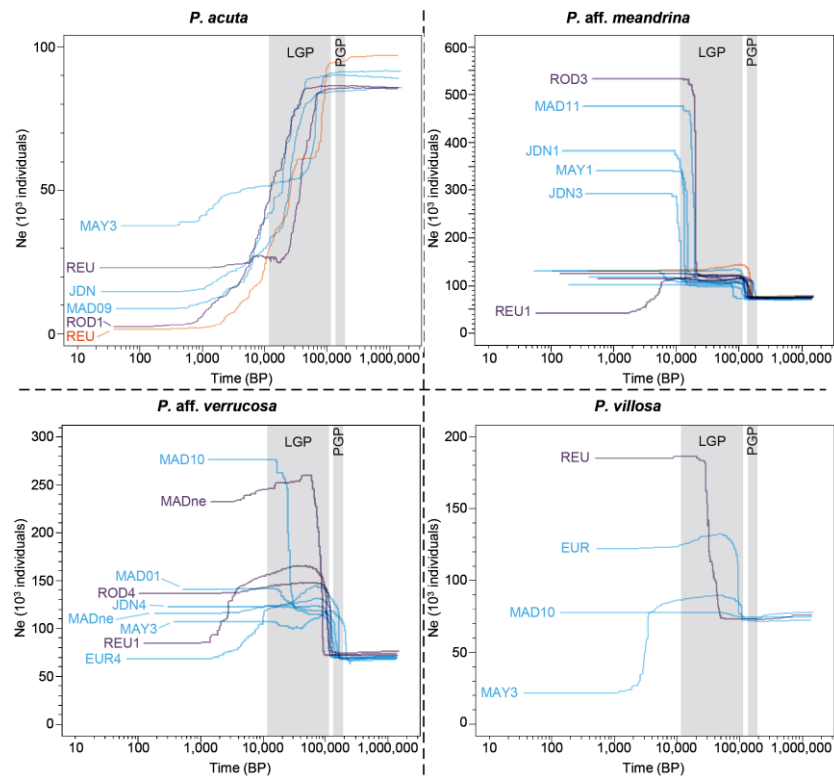
453 [2/3rd column] **Figure 4** Isolation by distance \times environment in *Pocillopora* species from the southwestern
 454 Indian Ocean (i.e., *P. acuta*, *Pocillopora* aff. *P. meandrina*, *Pocillopora* aff. *P. verrucosa* and *P. villosa* nomen
 455 *nudum*; indicated by a different symbol). First three principal components (PC1-3; percentages of variation
 456 explained in parentheses) of the factorial analysis of mixed data (FAMD) with within-species pairwise
 457 population F_{ST} , shortest distances at sea (Dist) and eight environmental variables: mean (M) and difference (D)
 458 in present mean surface temperature (SST), salinity (Salt), current velocity (CurVel) and chlorophyll
 459 concentration (Chloro). The correlation circle of these 10 quantitative variables is projected on the individual
 460 plot. Individuals (i.e., population pairs) are coloured differently depending on cluster assignments, as indicated
 461 by the table in the legend (e.g., comparisons between two populations belonging to a blue cluster are shown in
 462 blue). Non-coloured symbols indicate the qualitative variable “species”.
 463

464 Past effective population sizes

465 Past effective population size variations were very similar whether singletons were included or not.
 466 Therefore, here, we only present results without singletons, as they show fewer variations on small
 467 time scales and instead allow focusing on variation trends.

468 Except for *P. acuta*, similar ancestral variations of N_e through time were reconstructed among
 469 species. All populations from *P. aff. meandrina*, *P. aff. verrucosa* and *P. villosa* (it was less obvious
 470 for this latter species, probably due to smaller population sample sizes) thus showed an ancestral
 471 signature of population expansion between ca. 100,000 and 200,000 years ago, which coincides with
 472 the end of the penultimate glacial period (PGP; ca. 135,000-194,000 years ago; Colleoni, Wekerle,
 473 Näslund, Brandefelt, & Masina, 2016). This expansion brought the ancestral N_e from ca. 75,000 to
 474 125,000 individuals (Fig. 5; see Appendix S9, Fig. S9.13). However, recent variations were different
 475 among species and among populations within species. Some populations of *P. aff. meandrina* thus
 476 showed a second signature of population expansion between ca. 10,000 and 20,000 years ago, which
 477 coincides with the end of the last glacial period (LGP; ca. 11,700-115,000 years ago; Adams, Maslin,
 478 & Thomas, 1999), while other populations showed no variation or a decline between ca. 2,000 and
 479 5,000 years ago. Finally, for *P. acuta*, all populations showed a bottleneck between ca. 2,000 and

480 100,000 years ago, bringing N_e from ca. 90,000 to less than 40,000 individuals depending on the
 481 population (Fig. 5; see Appendix S9, Fig. S9.13).
 482



483 [2/3rd column] **Figure 5** Past effective population sizes (N_e) for each population (see Fig. 2 for the codes;
 484 colour refers to the cluster) of the four *Pocillopora* species from the southwestern Indian Ocean (i.e., *P. acuta*,
 485 *Pocillopora* aff. *P. meandrina*, *Pocillopora* aff. *P. verrucosa* and *P. villosa nomen nudum*). Only populations
 486 with divergent variations are labelled for *P. aff. meandrina* to lighten the figure. Grey areas indicate glacial
 487 periods (LGP: last glacial period: ca. 11,700-115,000 years ago; PGP: penultimate glacial period: ca. 135,000-
 488 194,000 years ago).
 489

490 DISCUSSION

491 Focusing on *Pocillopora* species from the southwestern Indian Ocean (SWIO), this study assesses
 492 the genetic structure of four species presenting different reproductive strategies and colonising
 493 various habitats using genome-wide SNPs. Our results highlighted a similar structuring pattern within
 494 each species suggesting weak connectivity between Madagascar and the Mascarene Islands
 495 ecoregions. Moreover, similar demographic histories were inferred among populations (except for
 496 *P. acuta*), potentially indicating that populations from these different species have met the same
 497 environmental constraints and reacted similarly. This should be considered in light of ongoing rapid
 498 climate change. Altogether, through a multi-species genomic approach, these results offer new
 499 insights to better understand the connectivity pattern in the SWIO and to implement effective
 500 conservation measures in a context of coral decline.

501 502 **Weak connectivity between Madagascar and the Mascarene Islands**

503 In this study, whichever the species considered, more than 90% of the colonies sampled in the
 504 Madagascar ecoregion were assigned to a single genetic cluster, while more than 90% of the colonies
 505 sampled in the Mascarene Islands were assigned to one or two distinct clusters restricted almost

506 exclusively to this ecoregion. This, together with other analyses (networks, F_{ST}), supports a clear
507 genetic structuring pattern, related to geography, in all four investigated *Pocillopora* species.

508 This difference among genetic structuring patterns was previously found using microsatellites
509 in a larger number of colonies (including colonies from this study; see Appendix S1, Table S1.1):
510 while high connectivity was reported for *P. aff. meandrina*, *P. aff. verrucosa* and *P. villosa* (SSH09a,
511 SSH13a and SSH13b in Oury et al., 2021, respectively), strong genetic differentiation was found
512 within *P. acuta* (PSH05; G elin, Pirog, et al., 2018), so as in this study. Noteworthy, for
513 *P. aff. meandrina*, the three sympatric clusters previously found in relatively similar proportions in
514 all sampled sites from the SWIO (SSH09a-1, SSH09a-2 and SSH09a-3 *sensu* G elin, Fauvelot, et al.,
515 2018) were not retrieved: this over-partitioning was caused by a single microsatellite locus (PV7). At
516 the level of SSH09a (i.e., *P. aff. meandrina*), general high connectivity among populations was found
517 at the scale of the SWIO, as for *P. aff. verrucosa* and *P. villosa*. The microsatellites used thus appear
518 not enough informative to detect subtle structuring patterns such as those found between the blue and
519 purple clusters in *P. aff. meandrina*, *P. aff. verrucosa* and *P. villosa* using genomic data, while
520 remaining efficient when patterns are more pronounced, such as in *P. acuta*. Genomic data thus
521 allows finer resolution of connectivity patterns, as previously suggested (e.g., Coscia et al., 2020; Lal,
522 Southgate, Jerry, & Zenger, 2016).

523 Weak connectivity was already reported between Madagascar and the Mascarenes for several
524 other taxa, including hydrozoans (Postaire, G elin, Bruggemann, & Magalon, 2017; Postaire, G elin,
525 Bruggemann, Pratlong, & Magalon, 2017), giant clams (Fauvelot et al., 2020), holoturians (Pirog et
526 al., 2019), brittle stars (Hoareau, Boissin, Paulay, & Bruggemann, 2013) and fishes (Muths, Tessier,
527 & Bourjea, 2015). Geographic distances (although no significant isolation by distance was found),
528 coupled with currents, likely explain this weak gene flow between both ecoregions. The SWIO
529 oceanic circulation is strongly influenced by the south equatorial current (SEC). The latter, going
530 from east to west, transports propagules from the Mascarenes to Madagascar. However, Madagascar
531 acts as a land barrier, deflecting currents (and propagules) to the south (= south-east Madagascar
532 current; SEMC;), and then to the east due to the Coriolis force, generating the south Indian subtropical
533 gyre (SISTG; Hancke, Roberts, & Ternon, 2014; Lutjeharms & Bornman, 2010; Schott & McCreary
534 Jr, 2001; Fig. 1), congruent with larval dispersal models (Crochelet et al., 2020; Gamoyo, Obura, &
535 Reason, 2019). Accordingly, asymmetric migration from the Mascarenes to the east coast of
536 Madagascar, a locality little sampled in our study, is expected to occur, something that could then be
537 tested using coalescent-based demographic simulations. Further studies, including samples from
538 eastern Madagascar, are thus needed to clarify the connectivity of the whole SWIO region.

539

540 **Habitats and reproductive strategies influence connectivity**

541 Although similar structuring patterns were found among SWIO populations for the four *Pocillopora*
542 species, the genetic differentiation was stronger (F_{ST} about 10 times higher) for *P. acuta*. This seems
543 related to intrinsic differences among species, and particularly to preferred habitats and reproductive
544 strategies.

545 *Pocillopora acuta* is mainly found in shallow (< 5 m depth) habitats, such as lagoons or flat
546 reefs (Veron, 2000), which are relatively enclosed. Conversely, the other species are found on outer
547 reef slopes in contact with the open ocean (Veron, 2000). Populations from *P. acuta* would therefore
548 be more prone to self-recruitment (see e.g., Pinsky, Palumbi, Andréfouët, & Purkis, 2012), leading to
549 the higher genetic differentiation found among them. Additionally, this species reproduces both
550 through sexual and asexual strategies (Gélin, Fauvelot, et al., 2017), with a high prevalence of clonal
551 propagation (e.g., Gélin, Fauvelot, et al., 2017; Gorospe & Karl, 2013; Torda, Lundgren, Willis, &
552 van Oppen, 2013a, 2013b), as found here. Although our sampling was not designed to study clonality,
553 several colonies of *P. acuta* belonged to the same clonal lineage (clonal richness, $R = 0.39$), compared
554 to other species ($R \geq 0.84$). Most colonies from the same clonal lineage were found in the same site,
555 and only few were found in different sites less than 40 km apart, confirming previous observations
556 (Gélin, Fauvelot, et al., 2017; Souter et al., 2009). Dispersal over hundreds or thousands of kilometres
557 of asexually produced larvae (Oury et al., 2019), and even more so of fragments, therefore appears
558 limited. Accordingly, genetic differentiation among *P. acuta* populations should be higher than in
559 other species for which clonal propagation is rarer.

560 Other species-specific differences could be responsible for the observed differences. For
561 instance, larval biology represents a key element of dispersal abilities. Differences in settlement
562 behaviour and competency periods among species could induce dispersal at greater or lesser scales.
563 In *P. damicornis*, planulae competent over 100 days were reported (Richmond, 1987), but this
564 duration remains unknown for other species.

565

566 **The Mascarenes as stepping stones for long-distance gene flow?**

567 For two species (*P. acuta* and *P. aff. meandrina*), colonies sampled in the Mascarenes were assigned
568 to two distinct and sympatric clusters (the purple and orange ones) strongly differentiated. These
569 clusters may represent distinct cryptic species or lineages that diverged recently and are found in
570 apparent sympatry but with depth or microhabitat differential distributions (as in *Seriatopora hystrix*;
571 van Oppen, Bongaerts, Underwood, Peplow, & Cooper, 2011). However, although not having precise
572 depth and habitat data for each sample, samples from the same site and assigned to the two clusters
573 were collected during the same dive and mixed in sampling order, suggesting no depth nor habitat-
574 dependent distribution.

575 The purple cluster found in *P. acuta* was previously detected in a study exploring species limits
576 within the genus using genomics (Oury et al., 2023; corresponding to GSH05c-2 therein).
577 Surprisingly, it was found genetically closer to *P. acuta* colonies from New Caledonia ecoregion than
578 to colonies of the SWIO. This may suggest an eastern origin of these colonies (central or eastern Indo-
579 Pacific), but the geographic distances involved appear too large, even through stepping-stones (Wood,
580 Paris, Ridgwell, & Hendy, 2014), for conventional gene flow (the distance between the Mascarenes
581 and western Australia is over 5,000 km). Indeed, weak connectivity was previously reported between
582 populations of *Pocillopora* corals from the Indian and Pacific Oceans (e.g., Gélin, Pirog, et al., 2018;
583 Oury et al., 2021), but also in hydrozoans (Postaire, Gélin, Bruggemann, & Magalon, 2017; Postaire,
584 Gélin, Bruggemann, Pratlong, et al., 2017), holothurians (Pirog et al., 2019) or starfishes (Otwoma &

585 Kochzius, 2016). Gene flow through passive oceanic rafting (Nikula, Spencer, & Waters, 2013) or
586 human movements (e.g., ballast waters, hull fouling; Gollasch, 2007) may be involved.

587 For *P. aff. meandrina*, the most genetically distant cluster was the orange one, restricted to
588 REU1, close to the main international seaport of Reunion Island. As no colonies were found admixed
589 between the orange and purple clusters, although being sympatric and supposedly belonging to the
590 same species (i.e., being interfertile), a recent colonisation (inducing limited reproduction events
591 between both clusters), through maritime transport, can be hypothesised. However, in this case, a
592 recent bottleneck effect should have been detected, whereas *Ne* variations of this population appear
593 similar to the others, whether singletons are considered or not. It is therefore unclear whether the
594 Mascarenes could represent stepping-stones for long-distance gene flow and complementary larger-
595 scale studies, including colonies from the northern and eastern Indian Ocean, are needed to confirm
596 the origin of these clusters. Noteworthy, should they represent distinct species, results and
597 interpretations of this study remain the same since analyses were performed on each cluster
598 separately.

599

600 **Shared demographic histories and constraints**

601 As genetic structuring patterns among *Pocillopora* species in the SWIO, ancestral demographic
602 histories were very similar, except for *P. acuta*. They suggested an expansion of all SWIO
603 populations from *P. aff. meandrina*, *P. aff. verrucosa* and *P. villosa* ca. 100,000 years ago, following
604 the penultimate glacial period (Colleoni et al., 2016), as previously found in *Acropora tenuis* (Cooke
605 et al., 2020; Mao et al., 2018). This period was characterised by a global warming of ocean
606 temperatures (Herbert, Peterson, Lawrence, & Liu, 2010), a sea level rise associated with the melting
607 of glaciers (Rohling et al., 1998, 2014), as well as an intensification of currents and a change in their
608 direction (Colleoni et al., 2016). Altogether, these changes probably induced the colonisation of new
609 habitats, and therefore demographic expansions.

610 More recently, demographic reconstructions diverged among populations, some showing an
611 expansion between ca. 10,000 and 20,000 years ago, following the last glacial maximum, while others
612 remained stable or showed a bottleneck over the same period. On one hand, these differences could
613 result from differential environmental constraints depending on the populations. For example,
614 changes in currents might both favour gene flow among some populations but increase the isolation
615 of others. However, demographic inferences differed between sympatric populations from different
616 species, questioning this hypothesis. On the other hand, differences could result from methodological
617 artefacts, as the number of SNPs used (see Appendix S9, Fig. S9.13) might be insufficient for
618 accurate demographic inferences (Excoffier, Dupanloup, Huerta-Sánchez, Sousa, & Foll, 2013;
619 Marchi, Schlichta, & Excoffier, 2021; Terhorst & Song, 2015).

620 Finally, concerning *P. acuta*, all populations showed a constant demographic decline for about
621 80,000 years which is probably related to the strong genetic structuring among populations (Heller,
622 Chikhi, & Siegismund, 2013; Lesturgie, Planes, & Mona, 2022). Inferred sizes of *P. acuta*
623 populations must nevertheless be interpreted cautiously, as representing the effective and not the real
624 population sizes. Consequently, a clonal lineage is considered as a single individual, whereas it could

625 be represented by dozens of colonies that are all able to reproduce sexually. Populations sizes of this
626 species are thus certainly underestimated, especially since the models on which demographic
627 inferences are based were not designed for clonal populations.

628 Thus, except for *P. acuta*, all *Pocillopora* populations from the SWIO showed similar
629 demographic signals, suggesting that they met the same environmental constraints and reacted in the
630 same way. This similar sensitivity to environmental changes among species should be taken into
631 account when implementing conservation measures, especially with ongoing climate change.

632

633 In conclusion, this study assesses for the first time the connectivity and demographic history of
634 four *Pocillopora* species from the SWIO using genome-wide SNPs. Genomic data refined the genetic
635 structuring patterns previously inferred using microsatellites and detected a weak connectivity
636 between Madagascar and the Mascarene Islands ecoregions. Moreover, this multi-species approach
637 highlighted different genetic structures likely linked to species-specific characteristics, such as
638 habitats and reproductive strategies. Similarly, demographic reconstructions highlighted shared
639 demographic histories (except for *P. acuta*), probably as populations from the different species shared
640 the same environmental constraints and reacted similarly. Altogether, these results suggest that the
641 four species of *Pocillopora* studied, especially *P. aff. meandrina*, *P. aff. verrucosa* and *P. villosa*,
642 show the same sensitivity to environmental changes. Their conservation must therefore be done as a
643 whole, with appropriate measures for each management unit (i.e., distinguishing Madagascar and the
644 Mascarene Islands ecoregions).

645

646 **ACKNOWLEDGEMENTS**

647 This work was supported in part through grants from the LabEx CORAIL (AI PocillopoRAD). All
648 permissions for fieldwork have been obtained from the relevant authorities. Coral sampling in the
649 north-east and north-west of Madagascar was carried out during the MAD
650 (<http://dx.doi.org/10.17600/16004700>) oceanographic campaign on board RV Antea (IRD; sampling
651 permit no. 16/1021-AE/SG/DAJC/ SAG/NAV/France). Sampling in Reunion Island was
652 supported by the program CONPOCINPA (LabEx CORAIL fund; sampling permit no. 14-
653 2013/DEAL/SEB/UBIO); in the south of Madagascar in collaboration with the Institut Halieutique
654 des Sciences Marines (Tulear; sampling permit no. 16/1040-AE/SG/DAJC/ SAG/NAV/France);
655 in Rodrigues with the collaboration of the Rodrigues Regional Assembly and the south-east Marine
656 Protected Area (sampling permit no. MU140897/Regional Assembly), supported by project
657 Biodiversity (POCT FEDER fund); in Europa, Juan de Nova, and Glorioso Islands by program
658 BIORECIE (financial supports from INEE, INSU, IRD, AAMP, FRB, TAAF, and the foundation
659 Veolia Environnement; sampling permits no. 2011-54/TAAF and no. 2013-66/TAAF); and in
660 Mayotte by program SIREME (FED; sampling permit no. 2016-31/DMSOI). HM thanks all the
661 buddies who helped with photographs during diving (J. Butscher, S. Andréfouët, L. Bigot, and
662 M. Pinault). We acknowledge the Plateforme iGenSeq of the Institut du Cerveau et de la Moelle
663 épinière (ICM, Paris, France) for library preparations and sequencing. Bioinformatics analyses were
664 performed on the Genotoul bioinformatics platform Toulouse Occitanie (Bioinfo Genotoul,

665 <https://doi.org/10.15454/1.5572369328961167E12>). NO was financially supported by a PhD contract
666 from the Doctoral School “Sciences, Technologies, Santé” of Reunion Island University.

667

668 CONFLICT OF INTEREST

669 The authors state that there is no conflict of interest.

670

671 DATA ACCESSIBILITY

672 Raw sequencing reads were deposited on the NCBI (BioProject PRJNA909966). All other data
673 underlying this article (metadata, VCF files, etc.) are available online
674 (<https://doi.org/10.5061/dryad.pnvx0k6vw>).

675

676 REFERENCES

- 677 Adams, J., Maslin, M., & Thomas, E. (1999). Sudden climate transitions during the Quaternary. *Progress in*
678 *Physical Geography*, 23(1), 1-36. <https://doi.org/10.1177/030913339902300101>
- 679 Assis, J., Tyberghein, L., Bosch, S., Verbruggen, H., Serrão, E. A., & De Clerck, O. (2018). Bio-ORACLE
680 v2.0 : Extending marine data layers for bioclimatic modelling. *Global Ecology and Biogeography*,
681 27(3), 277-284. <https://doi.org/10.1111/geb.12693>
- 682 Benzoni, F., Bianchi, C. N., & Morri, C. (2003). Coral communities of the northwestern Gulf of Aden
683 (Yemen) : Variation in framework building related to environmental factors and biotic conditions.
684 *Coral Reefs*, 22(4), 475-484. <https://doi.org/10.1007/s00338-003-0342-1>
- 685 Bosch, S., & Fernandez, S. (2023). *sdmpredictors : Species distribution modelling predictor datasets* [R].
686 <https://CRAN.R-project.org/package=sdmpredictors>
- 687 Bouwmeester, J., Coker, D. J., Sinclair-Taylor, T. H., & Berumen, M. L. (2021). Broadcast spawning of
688 *Pocillopora verrucosa* across the eastern and western coast of the central Red Sea. *Ecosphere*, 12(1),
689 03340. <https://doi.org/10.1002/ecs2.3340>
- 690 Buck-Wiese, H., Burgués, I., Medrano, A., Navarrete-Fernandez, T., Garcia, M., & Wieters, E. A. (2018).
691 Patterns in sexual reproduction of the dominant scleractinian corals at Rapa Nui (Easter Island) :
692 *Pocillopora verrucosa* and *Porites lobata*. *Aquatic Biology*, 27, 1-11.
693 <https://doi.org/10.3354/ab00691>
- 694 Clark, T. W. (1993). Creating and using knowledge for species and ecosystem conservation : Science,
695 organizations, and policy. *Perspectives in Biology and Medicine*, 36(3), 497-525.
696 <https://doi.org/10.1353/pbm.1993.0013>
- 697 Coelho, M. A. G., & Lasker, H. R. (2016). Larval dispersal and population connectivity in Anthozoans. In S.
698 Goffredo & Z. Dubinsky (Éds.), *The Cnidaria, Past, Present and Future* (p. 291-315). Cham:
699 Springer International Publishing. https://doi.org/10.1007/978-3-319-31305-4_19
- 700 Colleoni, F., Wekerle, C., Näslund, J.-O., Brandefelt, J., & Masina, S. (2016). Constraint on the penultimate
701 glacial maximum Northern Hemisphere ice topography (≈ 140 kyrs BP). *Quaternary Science*
702 *Reviews*, 137, 97-112. <https://doi.org/10.1016/j.quascirev.2016.01.024>
- 703 Cooke, I., Ying, H., Forêt, S., Bongaerts, P., Strugnell, J. M., Simakov, O., ... Miller, D. J. (2020). Genomic
704 signatures in the coral holobiont reveal host adaptations driven by Holocene climate change and reef
705 specific symbionts. *Science Advances*, 6(48), abc6318. <https://doi.org/10.1126/sciadv.abc6318>
- 706 Coscia, I., Wilmes, S. B., Ironside, J. E., Goward-Brown, A., O’Dea, E., Malham, S. K., ... Robins, P. E.
707 (2020). Fine-scale seascape genomics of an exploited marine species, the common cockle
708 *Cerastoderma edule*, using a multimodelling approach. *Evolutionary Applications*, 13(8),
709 1854-1867. <https://doi.org/10.1111/eva.12932>
- 710 Cowman, P. F., Quattrini, A. M., Bridge, T. C. L., Watkins-Colwell, G. J., Fadli, N., Grinblat, M., ... Baird,
711 A. H. (2020). An enhanced target-enrichment bait set for Hexacorallia provides phylogenomic
712 resolution of the staghorn corals (Acroporidae) and close relatives. *Molecular Phylogenetics and*
713 *Evolution*, 153, 106944. <https://doi.org/10.1016/j.ympev.2020.106944>
- 714 Crochelet, E., Barrier, N., Andrello, M., Marsac, F., Spadone, A., & Lett, C. (2020). Connectivity between
715 seamounts and coastal ecosystems in the Southwestern Indian Ocean. *Deep Sea Research Part II:*
716 *Topical Studies in Oceanography*, 176, 104774. <https://doi.org/10.1016/j.dsr2.2020.104774>

- 717 De Palmas, S., Soto, D., Ho, M.-J., Denis, V., & Chen, C. A. (2021). Strong horizontal and vertical
718 connectivity in the coral *Pocillopora verrucosa* from Ludao, Taiwan, a small oceanic island. *PLoS*
719 *ONE*, 16(10), 0258181. <https://doi.org/10.1371/journal.pone.0258181>
- 720 Dorken, M. E., & Eckert, C. G. (2001). Severely reduced sexual reproduction in northern populations of a
721 clonal plant, *Decodon verticillatus* (Lythraceae). *Journal of Ecology*, 89(3), 339-350.
722 <https://doi.org/10.1046/j.1365-2745.2001.00558.x>
- 723 Eddy, T. D., Cheung, W. W., & Bruno, J. F. (2018). Historical baselines of coral cover on tropical reefs as
724 estimated by expert. *PeerJ*, 6, 4308. <https://doi.org/10.7717/peerj.4308>
- 725 Excoffier, L., Dupanloup, I., Huerta-Sánchez, E., Sousa, V. C., & Foll, M. (2013). Robust demographic
726 inference from genomic and SNPdata. *PLoS Genetics*, 9(10), 1003905.
727 <https://doi.org/10.1371/journal.pgen.1003905>
- 728 Fauvelot, C., Zuccon, D., Borsa, P., Grulois, D., Magalon, H., Riquet, F., ... Bouchet, P. (2020).
729 Phylogeographical patterns and a cryptic species provide new insights into Western Indian Ocean
730 giant clams phylogenetic relationships and colonization history. *Journal of Biogeography*, 47(5),
731 1086-1105. <https://doi.org/10.1111/jbi.13797>
- 732 Frichot, E., & François, O. (2015). LEA : An R package for landscape and ecological association studies.
733 *Methods in Ecology and Evolution*, 6(8), 925-929. <https://doi.org/10.1111/2041-210X.12382>
- 734 Frichot, E., Mathieu, F., Trouillon, T., Bouchard, G., & François, O. (2014). Fast and efficient estimation of
735 individual ancestry coefficients. *Genetics*, 196(4), 973-983.
736 <https://doi.org/10.1534/genetics.113.160572>
- 737 Gamoyo, M., Obura, D., & Reason, C. J. C. (2019). Estimating connectivity through larval dispersal in the
738 western Indian Ocean. *Journal of Geophysical Research: Biogeosciences*, 124(8), 2446-2459.
739 <https://doi.org/10.1029/2019JG005128>
- 740 Gélín, P., Fauvelot, C., Bigot, L., Baly, J., & Magalon, H. (2018). From population connectivity to the art of
741 striping Russian dolls : The lessons from *Pocillopora* corals. *Ecology and Evolution*, 8(2),
742 1411-1426. <https://doi.org/10.1002/ece3.3747>
- 743 Gélín, P., Fauvelot, C., Mehn, V., Bureau, S., Rouzé, H., & Magalon, H. (2017). Superclone expansion,
744 long-distance clonal dispersal and local genetic structuring in the coral *Pocillopora damicornis* type
745 β in Reunion Island, South Western Indian Ocean. *PLoS ONE*, 12(1), 0169692.
746 <https://doi.org/10.1371/journal.pone.0169692>
- 747 Gélín, P., Pirog, A., Fauvelot, C., & Magalon, H. (2018). High genetic differentiation and low connectivity
748 in the coral *Pocillopora damicornis* type β at different spatial scales in the Southwestern Indian
749 Ocean and the Tropical Southwestern Pacific. *Marine Biology*, 165, 167.
750 <https://doi.org/10.1007/s00227-018-3428-6>
- 751 Gélín, P., Postaire, B., Fauvelot, C., & Magalon, H. (2017). Reevaluating species number, distribution and
752 endemism of the coral genus *Pocillopora* Lamarck, 1816 using species delimitation methods and
753 microsatellites. *Molecular Phylogenetics and Evolution*, 109, 430-446.
754 <https://doi.org/10.1016/j.ympev.2017.01.018>
- 755 Gollasch, S. (2007). Is ballast water a major dispersal mechanism for marine organisms? In W. Nentwig
756 (Éd.), *Biological Invasions* (p. 49-57). Berlin, Heidelberg: Springer. https://doi.org/10.1007/978-3-540-36920-2_4
- 758 Gorospe, K. D., & Karl, S. A. (2013). Genetic relatedness does not retain spatial pattern across multiple
759 spatial scales : Dispersal and colonization in the coral, *Pocillopora damicornis*. *Molecular Ecology*,
760 22(14), 3721-3736. <https://doi.org/10.1111/mec.12335>
- 761 Gray, J. S. (1997). Marine biodiversity : Patterns, threats and conservation needs. *Biodiversity and*
762 *Conservation*, 6, 153-175. <https://doi.org/10.1023/a:1018335901847>
- 763 Hancke, L., Roberts, M. J., & Ternon, J.-F. (2014). Surface drifter trajectories highlight flow pathways in the
764 Mozambique Channel. *Deep Sea Research Part II: Topical Studies in Oceanography*, 100, 27-37.
765 <https://doi.org/10.1016/j.dsr2.2013.10.014>
- 766 Heller, R., Chikhi, L., & Siegismund, H. R. (2013). The confounding effect of population structure on
767 Bayesian skyline plot inferences of demographic history. *PLoS ONE*, 8(5), 62992.
768 <https://doi.org/10.1371/journal.pone.0062992>
- 769 Herbert, T. D., Peterson, L. C., Lawrence, K. T., & Liu, Z. (2010). Tropical ocean temperatures over the past
770 3.5 million years. *Science*, 328(5985), 1530-1534. <https://doi.org/10.1126/science.1185435>
- 771 Hijmans, R. J. (2023). *raster : Geographic data analysis and modeling* [R]. [https://CRAN.R-](https://CRAN.R-project.org/package=raster)
772 [project.org/package=raster](https://CRAN.R-project.org/package=raster)

- 773 Hoareau, T. B., Boissin, E., Paulay, G., & Bruggemann, J. H. (2013). The Southwestern Indian Ocean as a
774 potential marine evolutionary hotspot : Perspectives from comparative phylogeography of reef
775 brittle-stars. *Journal of Biogeography*, *40*(11), 2167-2179. <https://doi.org/10.1111/jbi.12155>
- 776 Huson, D. H., & Bryant, D. (2006). Application of phylogenetic networks in evolutionary studies. *Molecular*
777 *Biology and Evolution*, *23*(2), 254-267. <https://doi.org/10.1093/molbev/msj030>
- 778 Johnston, E. C., Forsman, Z. H., Flot, J.-F., Schmidt-Roach, S., Pinzón, J. H., Knapp, I. S. S., & Toonen, R.
779 J. (2017). A genomic glance through the fog of plasticity and diversification in *Pocillopora*.
780 *Scientific Reports*, *7*(1), 5991. <https://doi.org/10.1038/s41598-017-06085-3>
- 781 Jombart, T. (2008). adegenet : A R package for the multivariate analysis of genetic markers. *Bioinformatics*,
782 *24*(11), 1403-1405.
- 783 Jombart, T., Devillard, S., & Balloux, F. (2010). Discriminant analysis of principal components : A new
784 method for the analysis of genetically structured populations. *BMC Genetics*, *11*(1), 94.
785 <https://doi.org/10.1186/1471-2156-11-94>
- 786 Kamvar, Z. N., Tabima, J. F., & Grünwald, N. J. (2013). Poppr : An R package for genetic analysis of
787 populations with clonal or partially clonal reproduction. *PeerJ*, *4*, 281.
788 <https://doi.org/10.7287/peerj.preprints.161v1>
- 789 Keenan, K., McGinnity, P., Cross, T. F., Crozier, W. W., & Prodöhl, P. A. (2013). diversity : An R package
790 for the estimation and exploration of population genetics parameters and their associated errors.
791 *Methods in Ecology and Evolution*, *4*(8), 782-788. <https://doi.org/10.1111/2041-210X.12067>
- 792 Kivelä, M., Arnaud-Haond, S., & Saramäki, J. (2015). EDENetworks : A user-friendly software to build and
793 analyse networks in biogeography, ecology and population genetics. *Molecular Ecology Resources*,
794 *15*(1), 117-122. <https://doi.org/10.1111/1755-0998.12290>
- 795 Kopelman, N. M., Mayzel, J., Jakobsson, M., Rosenberg, N. A., & Mayrose, I. (2015). CLUMPAK : A
796 program for identifying clustering modes and packaging population structure inferences across K.
797 *Molecular Ecology Resources*, *15*(5), 1179-1191. <https://doi.org/10.1111/1755-0998.12387>
- 798 Korneliusen, T. S., Albrechtsen, A., & Nielsen, R. (2014). ANGSD : Analysis of Next Generation
799 Sequencing Data. *BMC Bioinformatics*, *15*(1), 356. <https://doi.org/10.1186/s12859-014-0356-4>
- 800 Kruger, A., & Schleyer, M. H. (1998). Sexual reproduction in the coral *Pocillopora verrucosa* (Cnidaria :
801 Scleractinia) in KwaZulu-Natal, South Africa. *Marine Biology*, *132*(4), 703-710.
802 <https://doi.org/10.1007/s002270050434>
- 803 Lal, M. M., Southgate, P. C., Jerry, D. R., & Zenger, K. R. (2016). Fishing for divergence in a sea of
804 connectivity : The utility of ddRADseq genotyping in a marine invertebrate, the black-lip pearl
805 oyster *Pinctada margaritifera*. *Marine Genomics*, *25*, 57-68.
806 <https://doi.org/10.1016/j.margen.2015.10.010>
- 807 Lê, S., Josse, J., & Husson, F. (2008). FactoMineR : an R package for multivariate analysis. *Journal of*
808 *Statistical Software*, *25*(1). <https://doi.org/10.18637/jss.v025.i01>
- 809 Lesturgie, P., Planes, S., & Mona, S. (2022). Coalescence times, life history traits and conservation
810 concerns : An example from four coastal shark species from the Indo-Pacific. *Molecular Ecology*
811 *Resources*, *22*(2), 554-566. <https://doi.org/10.1111/1755-0998.13487>
- 812 Li, H., Handsaker, B., Wysoker, A., Fennell, T., Ruan, J., Homer, N., ... 1000 Genome Project Data
813 Processing Subgroup. (2009). The Sequence Alignment/Map format and SAMtools. *Bioinformatics*,
814 *25*(16), 2078-2079. <https://doi.org/10.1093/bioinformatics/btp352>
- 815 Liu, X., & Fu, Y.-X. (2020). Stairway Plot 2 : Demographic history inference with folded SNP frequency
816 spectra. *Genome Biology*, *21*(1), 280. <https://doi.org/10.1186/s13059-020-02196-9>
- 817 Lutjeharms, J. R., & Bornman, T. G. (2010). The importance of the greater Agulhas Current is increasingly
818 being recognised. *South African Journal of Science*, *106*(3-4), 1-4.
- 819 Magalon, H., Adjeroud, M., & Veuille, M. (2005). Patterns of genetic variation do not correlate with
820 geographical distance in the reef-building coral *Pocillopora meandrina* in the South Pacific.
821 *Molecular Ecology*, *14*(7), 1861-1868. <https://doi.org/10.1111/j.1365-294X.2005.02430.x>
- 822 Maggioni, D., Arrigoni, R., Seveso, D., Galli, P., Berumen, M. L., Denis, V., ... Montano, S. (2020).
823 Evolution and biogeography of the *Zanclaea*-Scleractinia symbiosis. *Coral Reefs*.
824 <https://doi.org/10.1007/s00338-020-02010-9>
- 825 Manni, F., Guérard, E., & Heyer, E. (2004). Geographic patterns of (genetic, morphologic, linguistic)
826 variation : How barriers can be detected by using Monmonier's algorithm. *Human Biology*, *76*(2),
827 173-190. <https://doi.org/10.1353/hub.2004.0034>
- 828 Mantel, N. (1967). The detection of disease clustering and a generalized regression approach. *Cancer*
829 *Research*, *27*, 209-220.

- 830 Mao, Y., Economo, E. P., & Satoh, N. (2018). The roles of introgression and climate change in the rise to
831 dominance of *Acropora* corals. *Current Biology*, 28(21), 3373-3382.e5.
832 <https://doi.org/10.1016/j.cub.2018.08.061>
- 833 Marchi, N., Schlichta, F., & Excoffier, L. (2021). Demographic inference. *Current Biology*, 31(6),
834 R276-R279. <https://doi.org/10.1016/j.cub.2021.01.053>
- 835 Matz, M. V., Trembl, E. A., Aglyamova, G. V., & Bay, L. K. (2018). Potential and limits for rapid genetic
836 adaptation to warming in a Great Barrier Reef coral. *PLoS Genetics*, 14(4), e1007220.
837 <https://doi.org/10.1371/journal.pgen.1007220>
- 838 Monmonier, M. S. (1973). Maximum-difference barriers : An alternative numerical regionalization method.
839 *Geographical Analysis*, 5(3), 245-261.
- 840 Muths, D., Tessier, E., & Bourjea, J. (2015). Genetic structure of the reef grouper *Epinephelus merra* in the
841 West Indian Ocean appears congruent with biogeographic and oceanographic boundaries. *Marine*
842 *Ecology*, 36(3), 447-461. <https://doi.org/10.1111/maec.12153>
- 843 Nei, M. (1972). Genetic distance between populations. *The American Naturalist*, 106(949), 283-292.
844 <https://doi.org/10.1086/282771>
- 845 Nei, M. (1973). Analysis of gene diversity in subdivided populations. *Proceedings of the National Academy*
846 *of Sciences*, 70(12), 3321-3323. <https://doi.org/10.1073/pnas.70.12.3321>
- 847 Nielsen, R., Korneliussen, T., Albrechtsen, A., Li, Y., & Wang, J. (2012). SNP calling, genotype calling, and
848 sample allele frequency estimation from new-generation sequencing data. *PLoS ONE*, 7(7), 37558.
849 <https://doi.org/10.1371/journal.pone.0037558>
- 850 Nikula, R., Spencer, H. G., & Waters, J. M. (2013). Passive rafting is a powerful driver of transoceanic gene
851 flow. *Biology Letters*, 9(1), 20120821. <https://doi.org/10.1098/rsbl.2012.0821>
- 852 Otwoma, L. M., & Kochzius, M. (2016). Genetic population structure of the coral reef sea star *Linckia*
853 *laevigata* in the western Indian Ocean and Indo-West Pacific. *PLoS ONE*, 11(10), 0165552.
854 <https://doi.org/10.1371/journal.pone.0165552>
- 855 Oury, N., G elin, P., & Magalon, H. (2020). Cryptic species and genetic connectivity among populations of
856 the coral *Pocillopora damicornis* (Scleractinia) in the tropical southwestern Pacific. *Marine Biology*,
857 167, 142. <https://doi.org/10.1007/s00227-020-03757-z>
- 858 Oury, N., G elin, P., & Magalon, H. (2021). High connectivity within restricted distribution range in
859 *Pocillopora* corals. *Journal of Biogeography*, 48(7), 1679-1692. <https://doi.org/10.1111/jbi.14104>
- 860 Oury, N., G elin, P., Mass e, L., & Magalon, H. (2019). First study of asexual planulae in the coral
861 *Pocillopora damicornis* type β SSH05c from the southwestern Indian Ocean. *Coral Reefs*, 38(3),
862 499-503. <https://doi.org/10.1007/s00338-019-01800-0>
- 863 Oury, N., G elin, P., Rajaonarivelo, M., & Magalon, H. (2022). Exploring the *Pocillopora* cryptic diversity :
864 A new genetic lineage in the Western Indian Ocean or remnants from an ancient one? *Marine*
865 *Biodiversity*, 52, 5. <https://doi.org/10.1007/s12526-021-01246-0>
- 866 Oury, N., No el, C., Mona, S., Aurelle, D., & Magalon, H. (2023). From genomics to integrative species
867 delimitation? The case study of the Indo-Pacific *Pocillopora* corals. *Molecular Phylogenetics and*
868 *Evolution*, 184, 107803. <https://doi.org/10.1016/j.ympev.2023.107803>
- 869 Padovan, A., Chick, R. C., Cole, V. J., Dutoit, L., Hutchings, P. A., Jack, C., ... Fraser, C. I. (2020).
870 Genomic analyses suggest strong population connectivity over large spatial scales of the
871 commercially important baitworm, *Australonuphis teres* (Onuphidae). *Marine and Freshwater*
872 *Research*, 71(11), 1549-1556. <https://doi.org/10.1071/MF20044>
- 873 Pante, E., Puillandre, N., Viricel, A., Arnaud-Haond, S., Aurelle, D., Castelin, M., ... Samadi, S. (2015).
874 Species are hypotheses : Avoid connectivity assessments based on pillars of sand. *Molecular*
875 *Ecology*, 24(3), 525-544. <https://doi.org/10.1111/mec.13048>
- 876 Pembleton, L. W., Cogan, N. O. I., & Forster, J. W. (2013). StAMPP : An R package for calculation of
877 genetic differentiation and structure of mixed-ploidy level populations. *Molecular Ecology*
878 *Resources*, 13(5), 946-952. <https://doi.org/10.1111/1755-0998.12129>
- 879 Pinsky, M. L., Palumbi, S. R., Andr efou et, S., & Purkis, S. J. (2012). Open and closed seascapes : Where
880 does habitat patchiness create populations with high fractions of self-recruitment? *Ecological*
881 *Applications*, 22(4), 1257-1267. <https://doi.org/10.1890/11-1240.1>
- 882 Pinz on, J. H., Sampayo, E., Cox, E., Chauka, L. J., Chen, C. A., Voolstra, C. R., & LaJeunesse, T. C. (2013).
883 Blind to morphology : Genetics identifies several widespread ecologically common species and few
884 endemics among Indo-Pacific cauliflower corals (*Pocillopora*, Scleractinia). *Journal of*
885 *Biogeography*, 40, 1595-1608. <https://doi.org/10.1111/jbi.12110>

- 886 Pirog, A., Latreille, A. C., Madelaine, C., Gélín, P., Frouin, P., & Magalon, H. (2019). High clonal
887 propagation and low population connectivity in the holothurian *Stichopus chloronotus* from the
888 Indo-Pacific. *Marine Biology*, 166(5), 63. <https://doi.org/10.1007/s00227-019-3512-6>
- 889 Postaire, B., Gélín, P., Bruggemann, J. H., & Magalon, H. (2017). One species for one island? Unexpected
890 diversity and weak connectivity in a widely distributed tropical hydrozoan. *Heredity*, 118(4),
891 385-394. <https://doi.org/10.1038/hdy.2016.126>
- 892 Postaire, B., Gélín, P., Bruggemann, J. H., Pratlong, M., & Magalon, H. (2017). Population differentiation or
893 species formation across the Indian and the Pacific Oceans? An example from the brooding marine
894 hydrozoan *Macrorhynchia phoenicea*. *Ecology and Evolution*, 7(20), 8170-8186.
895 <https://doi.org/10.1002/ece3.3236>
- 896 Pritchard, J. K., Stephens, M., & Donnelly, P. (2000). Inference of population structure using multilocus
897 genotype data. *Genetics*, 155(2), 945-959.
- 898 R Core Team. (2021). *R: a language and environment for statistical computing*. R Foundation for Statistical
899 Computing, Vienna, Austria. URL: <https://www.R-project.org/>.
- 900 Richmond, R. H. (1987). Energetics, competency, and long-distance dispersal of planula larvae of the coral
901 *Pocillopora damicornis*. *Marine Biology*, 93(4), 527-533. <https://doi.org/10.1007/BF00392790>
- 902 Ridgway, T., Hoegh-Guldberg, O., & Ayre, D. (2001). Panmixia in *Pocillopora verrucosa* from South
903 Africa. *Marine Biology*, 139(1), 175-181. <https://doi.org/10.1007/s002270100573>
- 904 Ridgway, T., Riginos, C., Davis, J., & Hoegh-Guldberg, O. (2008). Genetic connectivity patterns of
905 *Pocillopora verrucosa* in southern African Marine Protected Areas. *Marine Ecology Progress
906 Series*, 354, 161-168. <https://doi.org/10.3354/meps07245>
- 907 Robitzch, V., Banguera-Hinestroza, E., Sawall, Y., Al-Sofyani, A., & Woolstra, C. R. (2015). Absence of
908 genetic differentiation in the coral *Pocillopora verrucosa* along environmental gradients of the Saudi
909 Arabian Red Sea. *Frontiers in Marine Science*, 2, 5. <https://doi.org/10.3389/fmars.2015.00005>
- 910 Rohling, E. J., Fenton, M., Jorissen, F. J., Bertrand, P., Ganssen, G., & Caulet, J. P. (1998). Magnitudes of
911 sea-level lowstands of the past 500,000 years. *Nature*, 394(6689), 162-165.
912 <https://doi.org/10.1038/28134>
- 913 Rohling, E. J., Foster, G. L., Grant, K. M., Marino, G., Roberts, A. P., Tamisiea, M. E., & Williams, F.
914 (2014). Sea-level and deep-sea-temperature variability over the past 5.3 million years. *Nature*,
915 508(7497), 477-482. <https://doi.org/10.1038/nature13230>
- 916 Schmidt-Roach, S., Lundgren, P., Miller, K. J., Gerlach, G., Noreen, A. M. E., & Andreakis, N. (2012).
917 Assessing hidden species diversity in the coral *Pocillopora damicornis* from Eastern Australia.
918 *Coral Reefs*, 32(1), 161-172. <https://doi.org/10.1007/s00338-012-0959-z>
- 919 Schmidt-Roach, S., Miller, K. J., Lundgren, P., & Andreakis, N. (2014). With eyes wide open : A revision of
920 species within and closely related to the *Pocillopora damicornis* species complex (Scleractinia;
921 Pocilloporidae) using morphology and genetics. *Zoological Journal of the Linnean Society*, 170(1),
922 1-33. <https://doi.org/10.1111/zoj.12092>
- 923 Schmidt-Roach, S., Miller, K. J., Woolsey, E., Gerlach, G., & Baird, A. H. (2012). Broadcast spawning by
924 *Pocillopora* species on the Great Barrier Reef. *PLoS ONE*, 7(12), 50847.
925 <https://doi.org/10.1371/journal.pone.0050847>
- 926 Schott, F. A., & McCreary Jr, J. P. (2001). The monsoon circulation of the Indian Ocean. *Progress in
927 Oceanography*, 51(1), 1-123. [https://doi.org/10.1016/S0079-6611\(01\)00083-0](https://doi.org/10.1016/S0079-6611(01)00083-0)
- 928 Souter, P., Henriksson, O., Olsson, N., & Grahn, M. (2009). Patterns of genetic structuring in the coral
929 *Pocillopora damicornis* on reefs in East Africa. *BMC Ecology*, 9, 19. <https://doi.org/10.1186/1472-6785-9-19>
- 930 Sundqvist, L., Keenan, K., Zackrisson, M., Prodöhl, P., & Kleinhans, D. (2016). Directional genetic
931 differentiation and relative migration. *Ecology and Evolution*, 6(11), 3461-3475.
932 <https://doi.org/10.1002/ece3.2096>
- 933 Terhorst, J., & Song, Y. S. (2015). Fundamental limits on the accuracy of demographic inference based on
934 the sample frequency spectrum. *Proceedings of the National Academy of Sciences*, 112(25),
935 7677-7682. <https://doi.org/10.1073/pnas.1503717112>
- 936 Thomas, L., Underwood, J. N., Adam, A. A. S., Richards, Z. T., Dugal, L., Miller, K. J., & Gilmour, J. P.
937 (2020). Contrasting patterns of genetic connectivity in brooding and spawning corals across a remote
938 atoll system in northwest Australia. *Coral Reefs*, 39(1), 55-60. <https://doi.org/10.1007/s00338-019-01884-8>
- 939
940

- 941 Torda, G., Lundgren, P., Willis, B. L., & van Oppen, M. J. H. (2013a). Genetic assignment of recruits reveals
942 short-and long-distance larval dispersal in *Pocillopora damicornis* on the Great Barrier Reef.
943 *Molecular Ecology*, 22(23), 5821-5834. <https://doi.org/10.1111/mec.12539>
- 944 Torda, G., Lundgren, P., Willis, B. L., & van Oppen, M. J. H. (2013b). Revisiting the connectivity puzzle of
945 the common coral *Pocillopora damicornis*. *Molecular Ecology*, 22(23), 5805-5820.
946 <https://doi.org/10.1111/mec.12540>
- 947 Torres, A. F., Forsman, Z. H., & Ravago-Gotanco, R. (2020). Shifts in coral clonality along a gradient of
948 disturbance : Insights on reproduction and dispersal of *Pocillopora acuta*. *Marine Biology*, 167(11),
949 161. <https://doi.org/10.1007/s00227-020-03777-9>
- 950 van der Ven, R. M., Heynderickx, H., & Kochzius, M. (2021). Differences in genetic diversity and
951 divergence between brooding and broadcast spawning corals across two spatial scales in the Coral
952 Triangle region. *Marine Biology*, 168(2), 17. <https://doi.org/10.1007/s00227-020-03813-8>
- 953 van Oppen, M. J. H., Bongaerts, P., Underwood, J. N., Peplow, L. M., & Cooper, T. F. (2011). The role of
954 deep reefs in shallow reef recovery : An assessment of vertical connectivity in a brooding coral from
955 west and east Australia. *Molecular Ecology*, 20(8), 1647-1660. <https://doi.org/10.1111/j.1365-294X.2011.05050.x>
- 956 Veron, J. E. N. (2000). *Corals of the world*. Australia: Australian Institute of Marine Science.
- 957 Weir, B. S., & Cockerham, C. C. (1984). Estimating F-statistics for the analysis of population structure.
958 *Evolution*, 38(6), 1358-1370. <https://doi.org/10.1111/j.1558-5646.1984.tb05657.x>
- 959 Wood, S., Paris, C. B., Ridgwell, A., & Hendy, E. J. (2014). Modelling dispersal and connectivity of
960 broadcast spawning corals at the global scale. *Global Ecology and Biogeography*, 23(1), 1-11.
961 <https://doi.org/10.1111/geb.12101>
- 962

963

964 **SUPPORTING INFORMATION**

965 **Appendix S1** Correspondences with previous studies.

966 **Appendix S2** Detailed sampling and colonies distribution among clusters.

967 **Appendix S3** Datasets construction.

968 **Appendix S4** Species identification.

969 **Appendix S5** Clonal lineages identification.

970 **Appendix S6** Genetic structure analyses.

971 **Appendix S7** Direction and barrier to gene flow.

972 **Appendix S8** Isolation by distance.

973 **Appendix S9** Population demographic histories.

974

975 **BIOSKETCHES**

976 **Nicolas Oury** is PhD student interested in the evolutionary history, biogeography and population
977 connectivity of marine species, notably the scleractinian genus *Pocillopora*. This work emerged from
978 his PhD, supervised by **Hélène Magalon**, assistant professor at Reunion Island University. **Stefano**
979 **Mona** is assistant professor at the EPHE in Paris and a specialist in demographic inferences. All
980 authors are interested in biogeography, population demography and connectivity in marine
981 environments.

982

983 Author contributions: NO and HM designed the study; HM collected samples; NO and HM did lab
984 steps; NO analysed the results with helpful guidance from SM; NO wrote the original draft and all
985 authors reviewed and edited the manuscript.

986

987 **FIGURE LEGENDS**

988

989 **Figure 1** Sampling localities of *Pocillopora* colonies (dark and light greys indicate lands and coral reefs,
990 respectively). Sites are numerically identified from the island code: GLO: Glorioso Islands, MAY: Mayotte,
991 MAD: Madagascar, JDN: Juan de Nova Island, EUR: Europa Island, REU: Reunion Island and ROD:
992 Rodrigues. Major oceanic currents are indicated schematically: MC: Mozambique current, WMC: west
993 Madagascar current, AC: Agulhas current, NEMC: north-east Madagascar current, SEMC: south-east
994 Madagascar current, SEC: south equatorial current and SISTG: south Indian subtropical gyre (Hancke,
995 Roberts, & Ternon, 2014; Lutjeharms & Bornman, 2010; Schott & McCreary Jr, 2001).

996

997 **Figure 2** Population structure of each *Pocillopora* species (i.e., *P. acuta*, *Pocillopora* aff. *P. meandrina*,
998 *Pocillopora* aff. *P. verrucosa* and *P. villosa nomen nudum*). For each species (numbers of individuals and
999 SNPs of the corresponding dataset in parentheses), results from the three assignment methods (sNMF,
1000 STRUCTURE and DAPC) at the retained K ($K = 2$ for *P. aff. verrucosa* and *P. villosa*; $K = 3$ for *P. acuta* and
1001 *P. aff. meandrina*) are indicated above, as well as the corresponding cluster repartition below (grey portions
1002 represent individuals not assigned to the same cluster by all methods). Populations retained for further analyses
1003 are labelled (colour refers to the cluster; population size in parentheses). Dashed polygons represent pooled
1004 populations. N : number of colonies; MAY: Mayotte, JDN: Juan de Nova Island, EUR: Europa Island, MAD:
1005 Madagascar (nw: northwestern, ne: northeastern, sw: southwestern), REU: Reunion Island, ROD: Rodrigues.

1006

1007 **Figure 3** Direction and barrier to gene flow for each *Pocillopora* species (i.e., *P. acuta*, *Pocillopora* aff.
1008 *P. meandrina*, *Pocillopora* aff. *P. verrucosa* and *P. villosa nomen nudum*). Populations are coloured according
1009 to clusters. Arrows indicate gene flow above the filter threshold for which the network becomes fragmented
1010 (t ; indicated above, along with the numbers of populations, individuals and SNPs retained). Note that no arrows
1011 do not indicate the absence of gene flow. Red lines symbolise barriers (width proportional to support over
1012 1,000 bootstrap replicates).

1013

1014 **Figure 4** Isolation by distance \times environment in *Pocillopora* species from the southwestern Indian Ocean (i.e.,
1015 *P. acuta*, *Pocillopora* aff. *P. meandrina*, *Pocillopora* aff. *P. verrucosa* and *P. villosa nomen nudum*; indicated
1016 by a different symbol). First three principal components (PC1-3; percentages of variation explained in
1017 parentheses) of the factorial analysis of mixed data (FAMD) with within-species pairwise population F_{ST} ,
1018 shortest distances at sea (Dist) and eight environmental variables: mean (M) and difference (D) in present
1019 mean surface temperature (SST), salinity (Salt), current velocity (CurVel) and chlorophyll concentration
1020 (Chloro). The correlation circle of these 10 quantitative variables is projected on the individual plot. Individuals
1021 (i.e., population pairs) are coloured differently depending on cluster assignments, as indicated by the table in
1022 the legend (e.g., comparisons between two populations belonging to a blue cluster are shown in blue). Non-
1023 coloured symbols indicate the qualitative variable “species”.

1024

1025 **Figure 5** Past effective population sizes (N_e) for each population (see Fig. 2 for the codes; colour refers to the
1026 cluster) of the four *Pocillopora* species from the southwestern Indian Ocean (i.e., *P. acuta*, *Pocillopora* aff.
1027 *P. meandrina*, *Pocillopora* aff. *P. verrucosa* and *P. villosa nomen nudum*). Only populations with divergent
1028 variations are labelled for *P. aff. meandrina* to lighten the figure. Grey areas indicate glacial periods (LGP:
1029 last glacial period: ca. 11,700-115,000 years ago; PGP: penultimate glacial period: ca. 135,000-194,000 years
1030 ago).